Marine Biology (2024) 171:29
https://doi.org/10.1007/s00227-023-04344-8

ORIGINAL PAPER

Lophelia reefs off North and West Africa–Comparing environment and health

L. Buhl-Mortensen[1] · R. Houssa[2] · B. M'bengue[3] · E. S. Nyadjro[4] · D. Cervantes[1] · M. Idrissi[2] · E. Mahu[5] · A. S. Dia[3] · M. Olsen[1] · C. Mas[1] · M. Chierici[6]

Received: 30 November 2022 / Accepted: 31 October 2023

Abstract

The health status of cold-water coral reefs on the West African coast was investigated with the main objective of obtaining knowledge of the adaptive capacity of *Lophelia pertusa* to environmental stressors. Three coral sites were studied, in Northern Morocco, in the Morocco/Mauritania region (both in 2020) and, in the Ghana and Ivory coast region (visited in 2012, 2017, and 2019). Area cover of live colonies, explored through underwater videos, was used as an indicator of reef health and compared with the environmental variables: reef position, depth, water mass, temperature, dissolved oxygen concentration (DO), carbonate chemistry (pH, aragonite saturation (ΩAr), macronutrients and particles (visual). For a broader picture of the adaptations presented by *Lophelia* our results were compared with reefs in contrasting environments. Off Ghana and Mauritania healthy reefs (i.e., having areas with more than 20 % cover of live colonies) were found to reside at DO concentrations between 1.1 and 1.6 ml L^{-1}, in corrosive waters (pH 7.7 and ΩAr 1.0) with high nutrient concentrations. By contrast, the reefs off the North of Morocco, sitting in well-oxygenated waters with oversaturated ΩAr, had no or few live colonies. Our findings together with data from other studies show that *Lophelia* has a wide tolerance to hypoxia and acidification, and that in relation to climate change increased temperature and silting could pose more serious threats. These findings highlight the importance of continued studies of *Lophelia* reefs in contrasting environmental conditions to better understand their adaptation potential to climate change-related stressors.

Keywords Cold-water coral · *Lophelia* · West Africa · OMZ · Aragonite undersaturation

Introduction

Lophelia pertusa, synonymous with *Desmophyllum pertusum* (Addamo et al. 2016), is a cold-water Scleractinian coral found worldwide, and it is the major reef-forming coral in the North Atlantic (Davies and Guinotte 2011; Buhl-Mortensen et al. 2015a, b; 2016). The greatest density of *Lophelia* reefs known so far has been found along the Norwegian coast (Buhl-Mortensen et al. 2015a, b) but it occurs throughout the Atlantic and is present along the West African coast (Buhl-Mortensen et al. 2017; Wienberg et al. 2018, Hanz et al. 2019; Hebbeln et al. 2020). Globally, *Lophelia* reefs occur within a wide depth range (39–3380 m). Regionally, however, it occurs in narrower depth zones parallel to the shelf break, or the rim of offshore banks and seamounts. It is most common at 200–1000 m in oceanic water (35 S), with temperatures between 4 and 12 °C (Teichert 1958; Zibrowius 1980; Frederiksen et al. 1992). Under favorable conditions, *L. pertusa* can form reefs that are tens of meters

Responsible Regional Editor: Ciemon Frank Caballes.

✉ L. Buhl-Mortensen
lenebu@hi.no

1 Institute of Marine Research, Bergen, Norway

2 Institut National de Recherche Halieutique (INRH), Casablanca, Morocco

3 Institut Mauritanien de Recherches Océanographiques et des Pêches (IMROP), Nouadhibou, Mauritanie

4 NOAA Northern Gulf Institute, Mississippi State University, 1021 Balch Blvd, Stennis Space Center, MS 39529, USA

5 Marine Biogeochemistry, University of Ghana, Accra, Ghana

6 Institute of Marine Research, Framsenteret, Tromsø, Norway

Published online: 13 December 2023

tall and hundreds of meters long, offering a wide range of habitats to other organisms (Mortensen et al. 1995; Wheeler et al. 2007; Buhl-Mortensen et al. 2010).

Previous studies on cold-water corals have shown that physical environmental factors such as temperature, salinity, water velocity, substratum type and food availability are important drivers influencing the distribution of *Lophelia* reefs (Strømgren 1971; Frederiksen et al. 1992; Freiwald et al. 1999; Mortensen et al. 2001; Dodds et al. 2007; Dullo et al. 2008). Few studies include information on their chemical environment such as the dissolved oxygen (DO) concentration, and aragonite saturation state (ΩAr) in the water column which is an indicator of potential limitation to calcification for *Lophelia*. The response of *Lophelia* reefs to climate change impacts, such as warming, deoxygenation and ocean acidification (IPCC 2019) warrants further investigation.

Scientific literature on *Lophelia* reefs in Africa remains limited. Buhl-Mortensen et al. (2017) reported a substantial reef on the Ghana/Ivory Coast shelf, and Coleman et al. (2005) and Wienberg et al. (2018) documented multiple mounds off the coast of Mauritania. The characteristics of these West African reefs differ from those of the North Atlantic reefs. These reefs, situated in an area that experienced minimal change during the last ice age, have sustained ongoing growth. Additionally, they are marked by a significant oxygen minimum zone (OMZ). Nonetheless, there exists a deficiency of knowledge and data concerning carbonate chemistry in this African region. Such data are indispensable for describing the main state of ocean acidification, its variability, driving forces, and its impact on the condition of *Lophelia* reefs.

With the support of the Ecosystem Approach to Fisheries (EAF) Nansen program, multiple scientific surveys have been conducted to facilitate habitat mapping along the North-West (NW) African shelf and slope, as well as along Ghana-Ivory Coast. As part of these surveys, three cold-water coral sites were studied: two along the Morocco and Mauritania coastline and one along Ghana-Ivory Coast.

The data collected during these scientific surveys have enabled a comprehensive study of the coral reef sites, covering the continental shelf/slope of the Mauritania-Morocco coast and Ghana/Ivory Coast. Underwater videos and parameters such as landscape features (canyons/shelf-slope), depth, water masses, currents, temperature fluctuations, dissolved oxygen concentration, carbonate chemistry (pH, ΩAr), nutrient composition, and particle distribution have been assessed. The environmental conditions at reef sites were compared with the health status of reefs (level of cover of live and dead *Lophelia* colonies). The results from the study areas were compared with reports from other North Atlantic reefs. This comparative analysis of the health status of documented *Lophelia* reefs within highly divergent environmental contexts can offer valuable insights into their adaptive capacity to climate change. This study presents a rare insight into the range and spatial variability of ocean acidification state within this region, and its subsequent impact on the well-being of *Lophelia* coral reefs.

Methods and data

Study area

Multiple cruises were conducted in the years 2012, 2017, 2019, and 2020 in the NW Africa shelf and slope, as well as the Ghana-Ivory Coast region, aboard the Research Vessel (RV) Dr. Fridtjof Nansen (DFN) as part of the EAF Nansen Program. This program is the outcome of a collaborative effort involving two prominent Norwegian institutions: the Norwegian Agency for Development Cooperation (Norad) and the Institute for Marine Research (IMR) in Bergen, Norway, in partnership with the United Nations' Food and Agriculture Organization (FAO) and NW African countries. These surveys successfully documented three sites with cold-water coral formations: Area A in northern Morocco, Area B at the Morocco-Mauritania border, and Area C in the waters of Ghana and Ivory Coast (Fig. 1).

Oceanographically, the study area is influenced in the north by the Canary Current System (CCS), which extends from the Strait of Gibraltar to the south of Guinea-Bissau (Bakun 1990), and in the south by the Guinea Current System (GCS) extending from Cape López near the equator to Cape Palmas at 7° W longitude. With the exception of Area A, Area B and C are subjected to upwelling. The CCS, one of the world's four major upwelling ecosystems, is characterized by seasonal variability of the trade winds between winter and summer inducing pronounced coastal sea surface temperature (SST) anomalies with a high seasonal contrast, mainly in the southern part of the system (BenAzzouz et al. 2015; Arístegui et al. 2009; Barton et al. 2013). During the last three decades, the CCS has warmed above the permanent thermocline. The more marked warming tendencies are observed in the Senegalo-Mauritanian tropical sector (Kifani et al. 2018; Pörtner et al. 2014; Vélez-Belchí et al. 2015; deCastro et al. 2014; Lima and Wethey 2012; Stramma et al. 2008).

In the Canary Current system (CCS), the core of the Oxygen Minimum Zone (OMZ) extends to the surface, and the upwelling of older, oxygen-depleted waters with low dissolved oxygen (DO) content is typically accompanied by high concentrations of DIC (i.e., CO_2) and consequently, low ΩAr and pH levels. These conditions are expected to be enhanced as ocean acidification progresses due to the increase in atmospheric CO_2 (Kifani et al. 2018; Pörtner et al. 2014; IPCC 2019). The Guinea Current System (GCS)

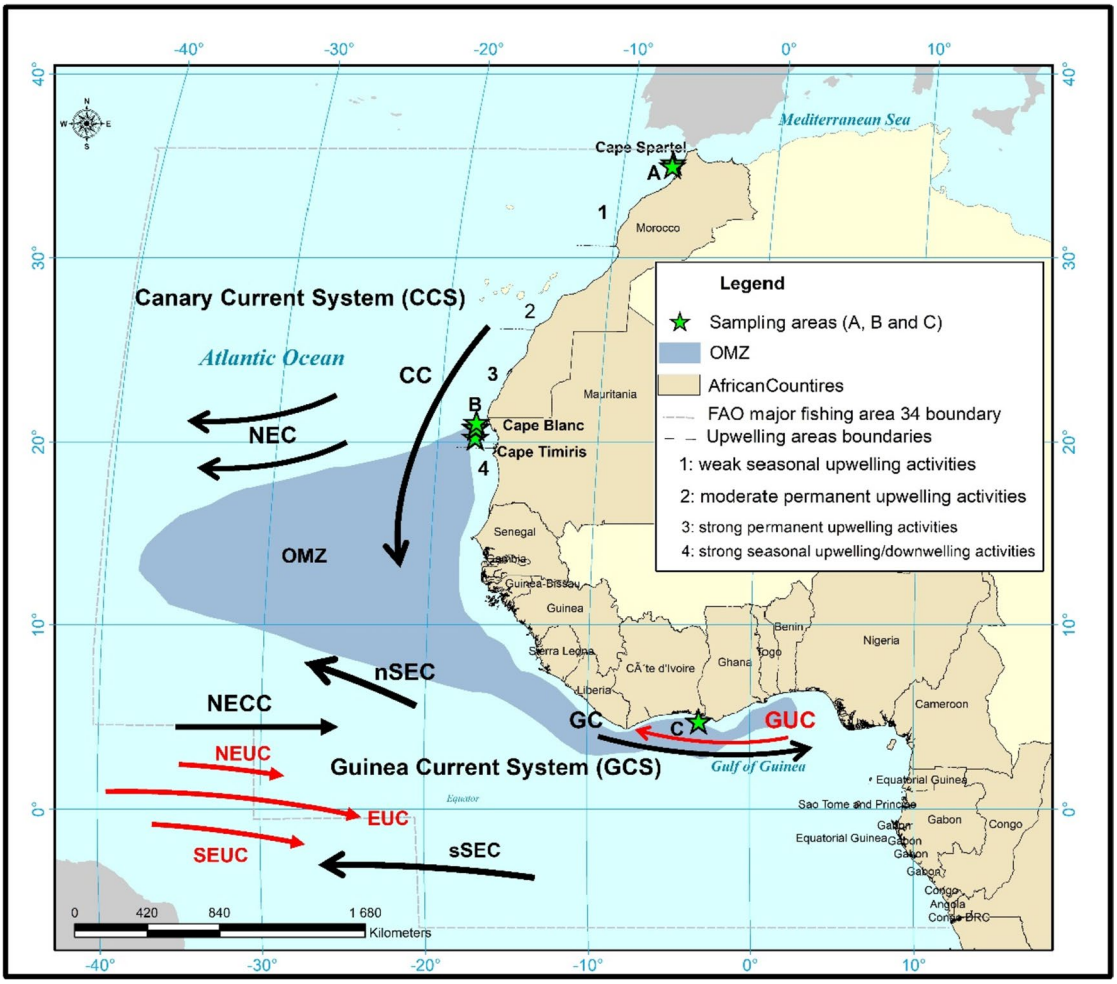

Fig. 1 Current systems and oceanographic features influencing the study areas: *CC*, Canary Current; *GC*, Guinea Current; *NEC*, North Equatorial Current; *NECC*, North Equatorial Countercurrent; *nSEC*, northern South Equatorial Current; *NEUC*, North Equatorial Undercurrent; *SEUC*, South Equatorial Undercurrent; *EUC*, Equatorial Undercurrent; *sSEC*, southern South Equatorial Current; *GUC* , Guinea Undercurrent; *OMZ*, Oxygen Minimum Zone. Green stars represent sampling areas

originates from two sources: the North Equatorial Countercurrent (NECC) and the Canary Current (CC), which flows into the Gulf of Guinea from the west-northwest (see Fig. 1). The Guinea Current (GC) follows an easterly path along the western coast of Africa at depths ranging from approximately 20 to 50 m, within the latitudinal range of 3°N to 5°N (Henin et al. 1986). As it enters the Gulf of Guinea, its velocities can reach nearly 100 cm/s near 5°W (Richardson and Reverdin 1987). The seasonal variability of the source currents plays a role in influencing the seasonal patterns of the Guinea Current. It experiences a minimum flow during the winter months (November–February) and a maximum flow during the summer months (May–September) (Ingham 1970). Notably, the GCS is characterized by areas of upwelling (Bakun 1978) and heightened biological productivity (Binet 1997). This upwelling is in geostrophic balance, with isotherms tilting upward towards the northern coast. As the current's intensity increases, this slope becomes steeper, bringing the thermocline closer to the coastal surface. Consequently, the coastal upwelling and the summer intensification of the Guinea Current are interconnected (Philander 1979). However, the Guinea Current stands out among upwelling regions due to the unique characteristic of exhibiting minimal correlation between sea surface temperature and wind patterns on a seasonal time scale. This suggests that remote factors, such as Kelvin waves, likely contribute to the dynamics of the region (Longhurst 1962; Bakun 1978).

Geomorphologically, Area A belongs to the "Strait of Gibraltar-Gulf of Cadiz" domain (Gibbons and Moreno 2002). It is characterized by a variety of geomorphological features (allochthones units, sediment wave, mega ripples, and mud volcanoes) that provide dynamic and diverse environments generating a variety of marine habitats (Agudo-bravo and Mangas 2015). In this zone, the continental shelf

is 40 to 50 km wide, the continental slope starts at 200 m and ranges from 1500 to 2000 m depth and the upwelling activities are seasonal (Fig. 1). Area B, is located on the border region between Morocco and Mauritania, between 21°N and 20°N. It is part of the Cape Blanc-Timiris Canyon landslide domain. The continental shelf is very wide as the result of strong sedimentation from an ancient paleo-river system (watershed, Tamanrasset); it extends to 140 km at the Banc d'Arguin. Between Cap Blanc and Cap Timiris, there are two groups of canyons, which converge at the foot of the slope and continue into the deep ocean (Agudo-Bravo and Mangas 2018). In this area, the upwelling activity is strong and permanent with a maximum intensity in summer and early fall (Fig. 1). Area C is situated on the upper continental slope at around 400 m depth in the vicinity of a canyon, and just off the narrow continental slope off Ghana at 4° 46 N and 3°09 W (Buhl-Mortensen et al. 2017). Generally, the configuration of the continental shelf is controlled by various breach systems that appear to extend to the edge of the slope (Cudjoe and Khan 1972). The region where the reef is located falls within the maximum width region, approximately 100 km offshore. The slope in this area is steep, extending seaward along an elongated and sediment-starved marginal ridge, the Ghana/Ivory Coast Marginal Ridge, which is aligned with the Romanche Fracture Zone. The reef is oriented perpendicular to the coast occurs within the depth range dominated by South Atlantic Central Water (SACW)–the source water mass that feeds the West African upwelling.

Oceanographic data

Data on hydrography and the chemical environment were collected during scientific cruises carried out by the FAO´s regional EAF Nansen program and the National Mauritanian marine-surveys program. During EAF Nansen surveys, vertical hydrography profiles and water sampling were conducted using a CTD-Rosette system with 12-niskin bottles. In 2019, four CTD surveys were performed in Area A and B, which provided a high resolution of physical and chemical conditions and supported the habitat mapping survey conducted on cruise 2020401. The summary of the sources with cruise ID, sampling dates, main study area, collected variables and survey program are listed in Supplementary information ESM 1.

CTD sensors for vertical profiles and water sampling

Hydrographical conditions were documented using a CTD (pressure) sensor (Seabird911, SBE3plus, SBE 4c) mounted to a 12-Niskin bottle Rosette. Additional sensors were mounted on the CTD-Rosette system for measurements of dissolved oxygen (DO) (SBE-53), chlorophyll fluorescence (WET Labs ECO-FL) and Photosynthetically Active Radiation (PAR, LOG CSW).

For validation and calibration of conductivity and DO sensors, water was collected from low-gradient depths at selected CTD stations for analysis. A Guildline Portasal Salinometer 8410A was used to measure the samples collected for conductivity (salinity), whereas the DO water samples were measured using a Metrohm 916 Ti-Touch potentiometric titrator performing automated Winkler titrations (Grasshoff et al. 1983). Additional water column hydrography data (salinity, temperature, DO) were collected along the Mauritania coast and shelf on cruises conducted by the Mauritanian Institute IMROP as part of their national monitoring surveys between 2010 and 2012 (Supplementary information ESM 1).

Determination of carbonate chemistry including pH and aragonite saturation

Water samples were collected and analyzed for pH and total alkalinity (AT) onboard following the general procedures described in Dickson et al. (2007). AT was determined using potentiometric titration (Metrohm) with 0.1 N hydrochloric acid in an open cell. Precision for AT was between ±2 and ±5 µmol kg $^{-1}$ based on triplicate analysis of each sample. The accuracy was controlled using Certified Reference Material (CRM) provided by Dickson laboratory (SIO, USA). pH was determined on a total scale using a spectrophotometric method and m-cresol purple as pH-sensitive indicator in a 1-cm pathlength quartz cuvette (Clayton and Byrne 1993). The perturbation from the indicator pH was corrected according to Chierici et al. (1999). The precision was between ±0.001 and ±0.005, based on triplicate measurements. The full carbonate chemistry including total dissolved inorganic carbon (DIC), ΩAr and in situ pH (pH_T), were calculated based on measured AT and pH, and CTD data using the carbonate system calculation program CO2SYS (Pierrot et al. 2006). The calculations were performed on the total hydrogen ion scale, using the carbonate system dissolution constants from Mehrbach et al. (1973) refit by Dickson and Millero (1987), and the hydrogen sulphate (HSO_4^-) dissociation constant of Dickson (1990). The concentration of calcium (Ca^{2+}) is assumed to be proportional to the salinity according to Mucci (1983; 10.28 × S/35 µmol kg^{-1}). The thermodynamic solubility products for aragonite and calcite (Ksp) are from Mucci (1983).

Nutrients

Seawater samples for nutrient analyses (nitrite, nitrate, silicate and phosphate) were collected at each water column sampling station in 20 ml polyethylene vials. Samples were preserved with 0.2 ml chloroform and kept refrigerated and

dark until being sent to the Institute of Marine Research (IMR), Bergen, Norway for analysis. Analyses were performed using a Skalar San++ Continuous Flow Analyser while following the procedures explained in detail by Gundersen et al. (2022).

Surface ocean data from remotely sensed resources

We obtained daily sea surface temperature (SST) data on a 0.25° × 0.25° grid from the National Oceanic and Atmospheric Administration (NOAA) National Centers for Environmental Information (NCEI) Optimum Interpolation Sea Surface Temperature (OISST) v2.1 product. The OISST product is produced by combining observations from ship measurements, Argo floats, buoys, and satellites (e.g., from the Advanced Very High-Resolution Radiometer -AVHRR-infrared satellite) (Reynolds et al. 2007). Six-hourly Ocean gap-free 0.25° × 0.25° gridded surface wind data were obtained from the Remote Sensing Systems' (RSS) Cross-Calibrated Multi-Platform (CCMP) v2.0 product (Mears et al. 2019). This product is produced by combining cross-calibrated satellite microwave winds and instrument observations. Surface velocity currents at a spatial resolution of 1° × 1° and representing mean currents in the upper 30 m of the ocean were obtained from the Ocean Surface Current Analyses Real-Time (OSCAR) data set (Bonjean and Lagerloef 2002). OSCAR currents are produced by combining satellite-derived ocean surface heights, surface winds, and SST using a diagnostic model of ocean currents based on frictional and geostrophic dynamics. Monthly mean values are computed from daily mean values. Seasonal anomalies were computed as the difference between monthly climatologies and the data mean, where means are computed over the common period of the datasets (i.e., January 1988–December 2020).

Visual mapping of reef sites

In total twelve video transects targeting coral reefs were conducted (Table 1 and Fig. 3), three in Area A and six in Area B in 2020 at cruise 2020401, and three in Area C in 2012 on cruise 2012407 targeting a large reef off Ghana. The positioning of video transects was selected based on bathymetry and acoustic backscatter gained from prior multibeam mapping. Positions, depth range and length of the video transects are provided in Table 1.

The video transect surveys were conducted using a Remotely Operated Vehicle (ROV) that is part of the IMR Video Assisted Multi Sampler (VAMS) (Buhl-Mortensen et al. 2017). During dives, the VAMS was towed by the DFN vessel at a speed of ~0.3 knots, and the ROV was remotely driven in front of VAMS. The benthic community components of the seabed encountered during video recording were annotated using the "CampodLogger" program developed by IMR. It allows for selecting bottom types from a drop-down menu while entering taxon names and comments manually. These entries are automatically 'tagged' with date, time, depth (both from the ship's echosounder and the ROV depth sensor), latitude and longitude (from both the ship and the ROV). The annotated occurrences of coral skeletons (rubble and blocks) and live *Lophelia* colonies were together with the bathymetry, used to identify coral reefs and their extent. The occurrence and cover of live coral colonies were used as an indicator of reef status as follows: "Dead" when no live colonies were observed, "Poor" when live coral colonies were present but never covered more than 5%, and "Healthy" when there were areas with a cover of live coral colonies

Table 1 Sampling information for the 12 video transect surveys conducted on mounds and coral reefs off West Africa by R/V Dr. Fridtjof Nansen including station number, date, start and stop positions, depth range and length of the transect (see also Fig. 3)

Area	Station	Date	START						STOP						Depth range	Transect length
			Deg	Min		Deg	Min		Deg	Min		Deg	Min		(m)	(m)
A	A5-7	18.02.2020	35	10.673	N	6	46.415	W	35	10.526	N	6	46.198	W	679–696	430
	A5-8	19.02.2020	35	00.141	N	6	48.882	W	34	59.910	N	6	48.900	W	574–675	400
	A5-9	19.02.2020	34	51.335	N	6	45.892	W	34	51.266	N	6	46.087	W	169–245	400
B	B6-1B	01.02.2020	20	14.798	N	17	40.200	W	20	14.227	N	17	40.250	W	486–597	1200
	B6-2	02.02.2020	20	14.996	N	17	42.380	W	20	15.174	N	17	42.288	W	520–581	280
	B6-3	03.02.2020	20	45.862	N	17	42.262	W	20	45.974	N	17	42.091	W	452–542	300
	B6-3B	03.02.2020	20	45.850	N	17	42.702	W	20	45.892	N	17	42.727	W	533–551	300
	B6-4	03.02.2020	20	48.326	N	17	42.281	W	20	48.173	N	17	42.263	W	503–575	300
	B6-5	03.02.2020	21	04.325	N	17	40.699	W	21	04.196	N	17	40.581	W	489–583	300
C	219	17.11.2012	4	45.681	N	3	09.181	W	4	45.850	N	3	09.253	W	385–423	277
	312	23.11.2012	4	45.846	N	3	09.246	W	4	46.231	N	3	08.819	W	375–442	349
	313	23.11.2012	4	46.237	N	3	08.816	W	4	46.361	N	3	08.379	W	373–402	275

exceeding 20%. The presence of trawl marks was used as an indicator of physical damage from fisheries.

Results

Water mass distribution

Three water masses can be identified off the coasts of Mauritania and Morocco (Figs. 1 and 2): South Atlantic Central Water (SACW), Eastern North Atlantic Central Water (ENACW) and Mediterranean Intermediate Water (MIW) (Fig. 2). In the upper water layer, the SACW and ENACW are dominant, with the well-oxygenated ENACW mixing with the salty sub - 11°C MIW coming from the Strait of Gibraltar (Area A). A frontal zone is located off Cape Blanc at 21°N (Area B) that separates the SACW and ENACW where mixing occurs. The ENACW has a salinity maximum of 36.7 PSU, whereas the SACW has a lower salinity maximum of 35.8 PSU (Emery 2001). The less saline SACW of Area B is also characterized by its DO deficiency with concentrations just above 1 ml L^{-1} qualifying as a pronounced oxygen minimum zone (OMZ) (Glessmer et al. 2009). SACW is also rich in nutrients and, exhibits a linear temperature–salinity relationship. During the survey, the measured temperature range in the vicinity of the coral reef was 8.5–9 °C and the salinity range was 34.8–34.85 psu. The water surrounding the Ghana reef (Area C) (Fig. 2) is mostly dominated by SACW with its characteristic temperature between 5°C and 18°C and salinity between 34.3 and 35.8 PSU (Emery 2001). However, it is only the low DO concentration of the SACW below 1.5 ml L^{-1} between 300 and 500 m that can be observed near the Ghana reef. The SACW can be seen mixing with the Antarctic Intermediate Water (AAIM) at 550 m where salinity and DO concentrations begin to increase.

Characteristics of reef sites and coral status

Area A

In Area A, off the northern Moroccan Atlantic coast, the observed corals are located around 35° N, between 200 and 700 m depth (Fig. 3a). In this Area, three video transect surveys were conducted at structures that potentially could be coral reefs. Table 2 and Supplementary information ESM 2 provide, respectively, information on coral observations and bathymetry of the surroundings of the coral mounds including the position of the video transects. Three transects showed remnants of coral reefs buried in the sediments and with few visible coral skeletons (Table 2 and Supplementary information ESM 2) and Fig. 4 presents examples of coral observations from the transects. On the mound at station A5-7, a 430 m long transect was conducted at 692 to 700 m depth uncovering soft bottom with coral skeletons occurring in depressions. Bathymetry revealed several mounds indicating the presence of a silted large coral reef. A 400 m long transect was conducted at A5-8 on the continental slope at 574 to 661 meters depth (Supplementary information ESM 2). The detailed bathymetry reveals a large reef area with several visible mounds. The dense occurrence of rubble and coral blocks with few signs of silting indicates that the reef died relatively recent. The 400-meter-long transect carried out at A5-9 spanned depths of 169 to 245 m on a shallow mound characterized by bathymetric features suggesting the presence of a submerged reef that is entirely covered by sediment. The observations revealed a mixed sediment setting consisting of gravel, bedrock and boulders, and 47% soft sediment. Coral rubble and blocks that look old, gray colored and corroded, are present at 213-243 meters depth.

Area B

In Area B, the observed corals were located between 21°N and 20°N (Fig. 3b) at a depth between 400 m and 600 m. Six video transect surveys were recorded on mounds that indicating the presence of reefs (B6-1 to B6-5) (Supplementary information ESM 3). At all mounds, "coral rubble" and/or "coral blocks" were observed and live *Lophelia* coral were found on three of these (Table 2; Supplementary information ESM 3 and Figs. 4, 5, 6, 7). Further north the targeted mounds were dead reefs with coral rubble scattered over large areas, while lost fishing gear and trawl marks indicated damage by trawling. On the mound at station B6-1, a 1200 m long video transect was conducted covering depths from 526 to 590 m. Here, large areas of healthy and living *L. perstusa* colonies were observed on a 70 m tall reef situated on the side of a canyon (Figs. 3b, 4d, 5). At station B6-2, a 280 m long video transect, was conducted on a 50 m tall and 350 m long reef, situated at 538 to 573 m depth. This reef had only a few scattered live *L. pertusa* colonies and large blocks of dead corals dominating the summit of the reef (Figs. 4e, 6). On the mound at station B6-3, a ~300 m long video transect was conducted at 453 to 540 m depth on a reef, that consisted mainly of dead corals. Only a single small colony of live *L. pertusa* was observed in an area with many coral blocks (Figs. 4f, 7). On a small mound near the larger reef at B6-3, at station B6-3B, a ~300 m long video transect was conducted between 536 and 560 m depth (Fig. 7, Supplementary information ESM 3; ESM 4). Some coral rubble was observed but no live colonies. On the mound at B6-4 a ~300 m long transect was conducted between 503 and 569 m depth, here large areas were covered with coral rubble and no live colonies were found (Supplementary information

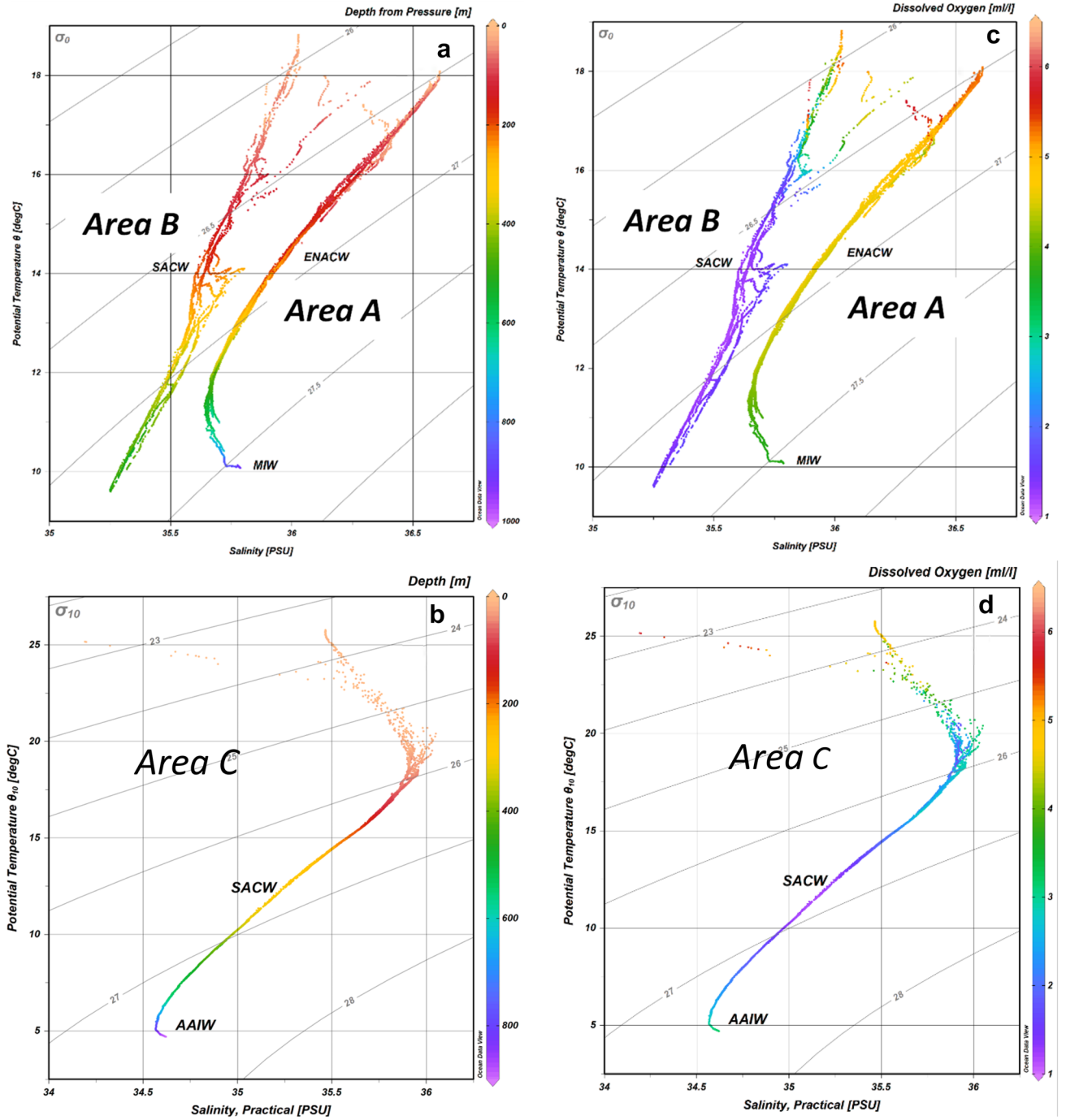

Fig. 2 Properties of the main water masses off the coasts of Morocco (Area A), Mauritania (Area B) and Ghana (Area C). **a** and **b** based on depth as indicated with color scale to the right. **c** and **d** based on dissolved oxygen concentration (ml L^{-1}) as indicated with color scale to the right. The water masses are: South Atlantic Central Water (SACW), Eastern North Atlantic Central Water (ENACW), Mediterranean Intermediate Water (MIW), and Antarctic Intermediate Waters (AAIW)

EMS 3; ESM 4). At station B6-5 a transect was conducted from 492 to 583 m depth on a mound that was partly covered with a thick layer of coral rubble (Supplementary information EMS 3; ESM 4).

Area C

The location of the Ghana reef site is shown in Fig. 2c. The multibeam bathymetric mapping conducted in 2009 indicates that the reef is 70 m high and1400 m long and

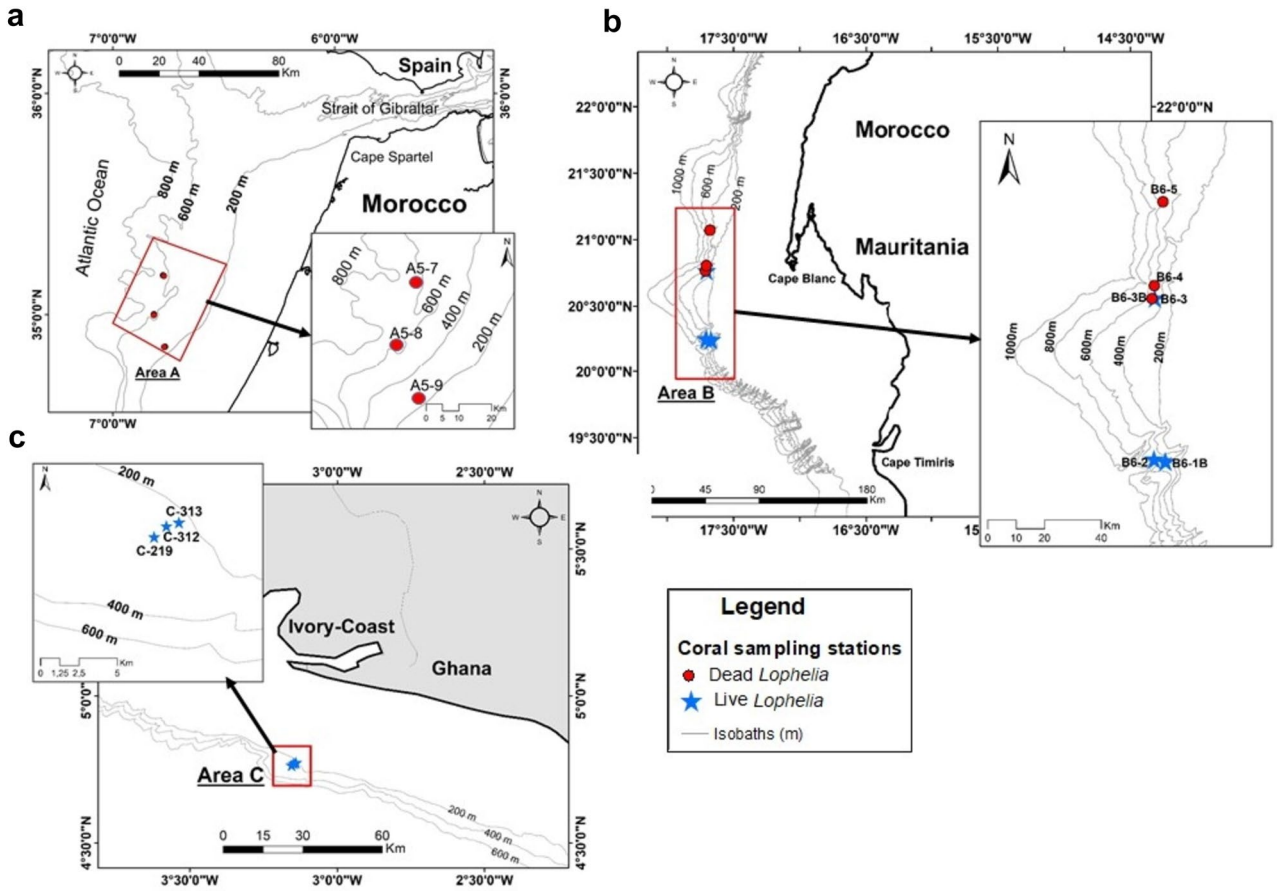

Fig. 3 Bathymetry map with isobaths showing coral reef sites. **a**. Area A north of Morocco. **b**. Area B around Morocco-Mauritania. **c**. Area C the Ghana reef at the Ghana-Ivory coast. Red dot: Reef with no live coral colonies. Blue stars: Reefs with live colonies

Table 2 Depth (m) range of *Lophelia* occurrences at the 12 video transects conducted on mounds and coral reefs of West Africa in areas A, B and C by RV-DFN. Coral presence is listed as the depth range of Dead coral (rubble and blocks), Dead blocks, Live colony cover. less than 5%, 5 to 20%, and more than 20%

Area	Station	Dead coral	Dead blocks	Live <5%	Live 5–20%	Live >20%	Trawl marks	Fishing gear	Reef status
	A5-7	692–700					x		Dead
A	A5-8	574–661	580–583				x		Dead
	A5-9	213–243	213–228				x	x	Dead
	B6-1B	515–597		559–597		538–562			Healthy
	B6-2	535–576		525–536				x	Poor
B	B6-3	454–536	457–511	469–515			x	x	Poor
	B6-3B	538–554					x	x	Dead
	B6-4	505–585					x	x	Dead
	B6-5	490–577	519–556				x		Dead
	219	385–423	385–423	385–403					Poor
C	312	374–442	374–428		374–428	375–377			Healthy
	313	373–402	373–393		373–375	375–374			Healthy

The occurrence of trawl marks and fishing gear at the stations is marked with x. Reef status is indicated as: Dead: only coral skeleton present, Poor: live corals covering < 5% in any area along the transect, Healthy: areas with a coral cover off > 20%

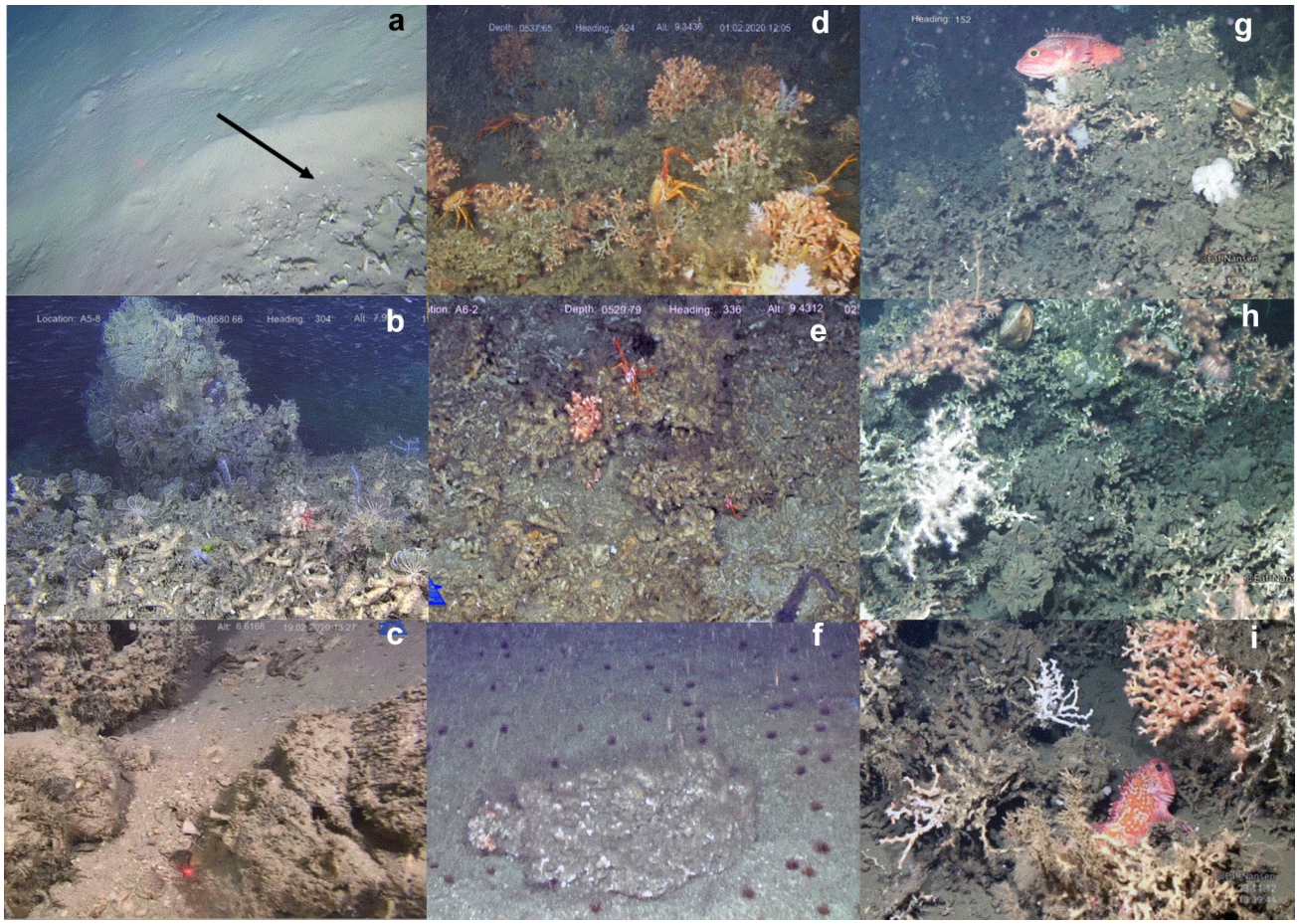

Fig. 4 Photos from the video transect surveys conducted on coral reefs, for positions of transects see Table 1 and Supplementary EMS 1–3. From Area A: **a**. At A5-7 coral rubble on top of a mound (black arrow) was buried under soft sediment. **b**. At A5-8 a thick carpet of coral rubbles and blocks indicating an old reef. **c**. At A5-9 at a reef almost totally covered by sediment with coral blocks and debris. From Area B: **d**. At B6-1 photo from an area with > 30 % cover of live L. pertusa colonies from a 70 m tall and healthy reef with a rich fauna. **e**. At B6-2 a thick cover of coral skeletons and blocks was present together with a few live colonies of L. pertusa. **f**. At B6-3 a small colony of live L. pertusa was found on a dead coral block (see also Fig. 5, 6, 7). At B6-3B, B6-4 and B6-5 dead reefs with coral rubble was observed (see Supplementary information EMS 4). From Area C at the large Ghana reef live L. pertusa colonies and a rich associated fauna was observed: **g**. from station 219. **h**. station 312 at the sumit of the reef. **i**. at station 313 (see Fig. 8 for details on video transect surveys)

around 250 m wide at the base. In this Area C, a large and healthy reef was located on the outer shelf on the eastern side of a canyon to the right side (Figs. 4g–i, 8). This 70 m high and 1400 m long reef is curve-shaped and located at 400 m depth. All three video transect surveys (219, 312, and 313) that were conducted on the reef showed the presence of healthy and live corals from 375 to 428 meters depth (Table 2).

Physical and chemical environment of the water column in the NW Africa reef sites

Area A

In Area A temperature, salinity, DO, chlorophyll a fluorescence (Chl a), pH and aragonite saturation (ΩAr) decreased from surface to bottom, while total dissolved

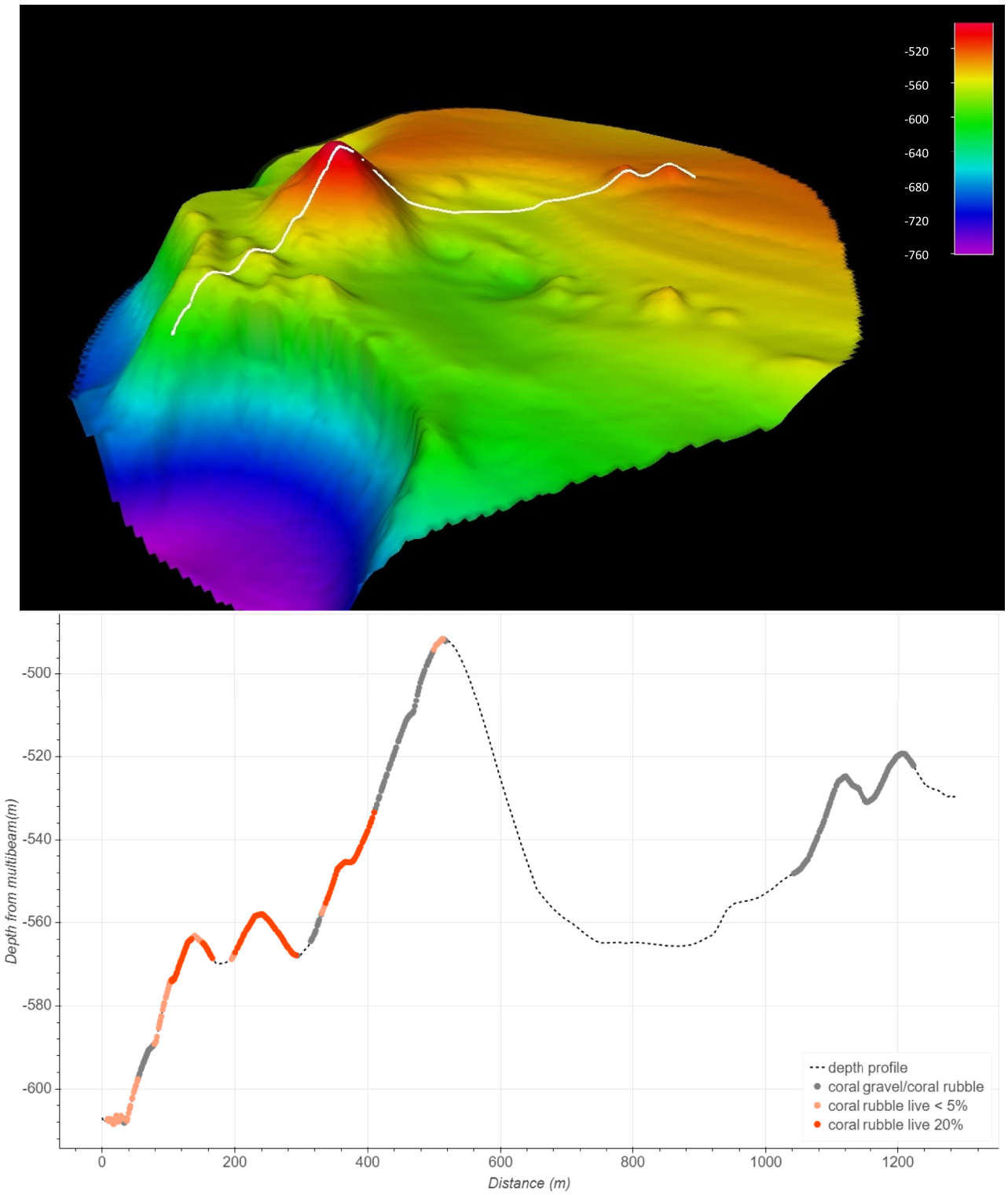

Fig. 5 In Area B the video transect survey at station B6-1 revealed a 70 m tall live and healthy Lophelia reef. Above: the position of the transect is marked as a white line on a 3D bathymetry map (colors indicating depth). Below: the depth profile of the transect with the presence of Lophelia along the transect

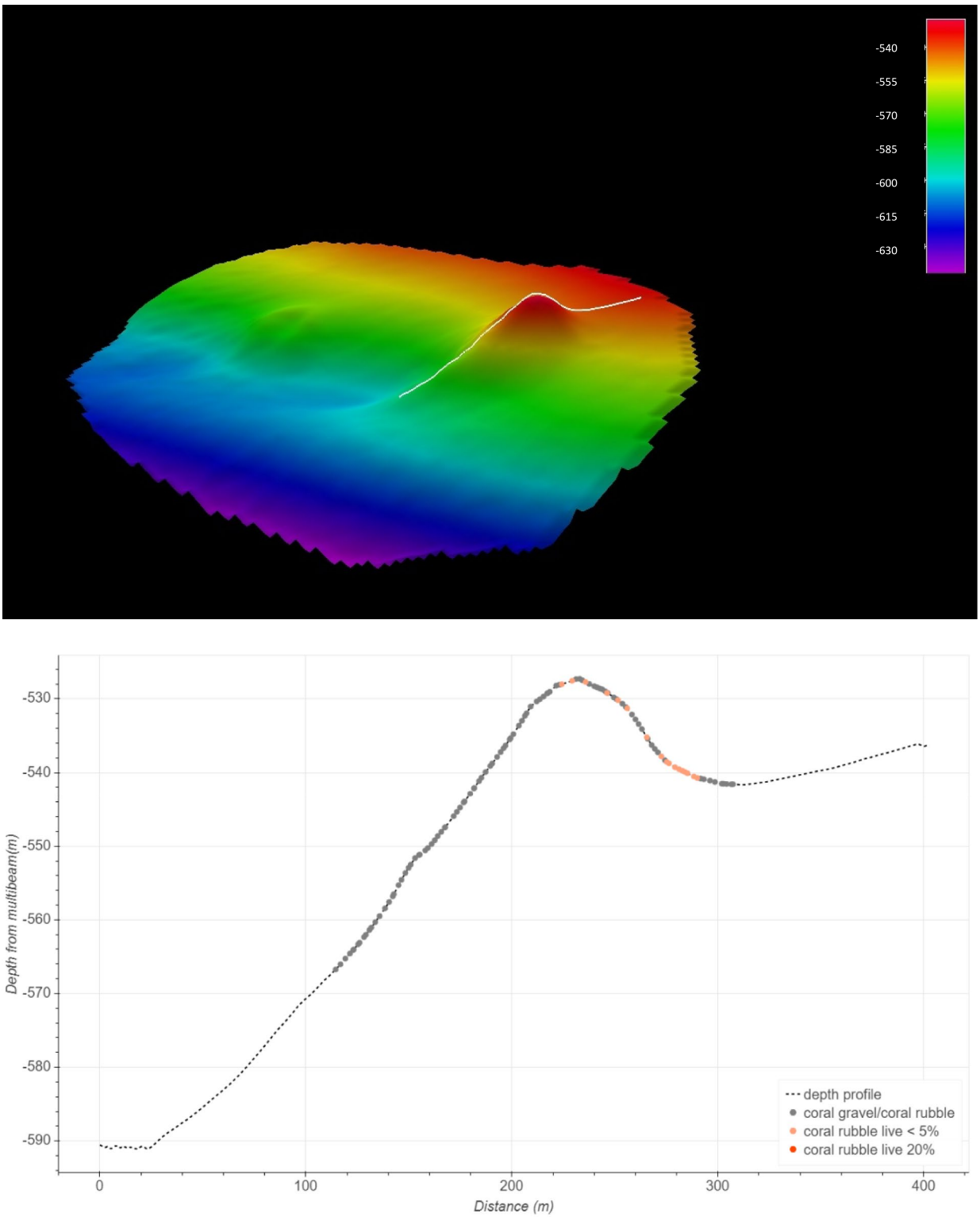

Fig. 6 In Area B the video transect survey at station B6-2 showed a reef with a few live corals. Above: the position of the transect is marked as a white line on a 3D bathymetry map colors indicating depth. Below: the depth profile of the transect with the presence of Lophelia. Dashed line: no corals observed. Only a few colonies of live corals were observed, for details see Fig. 4

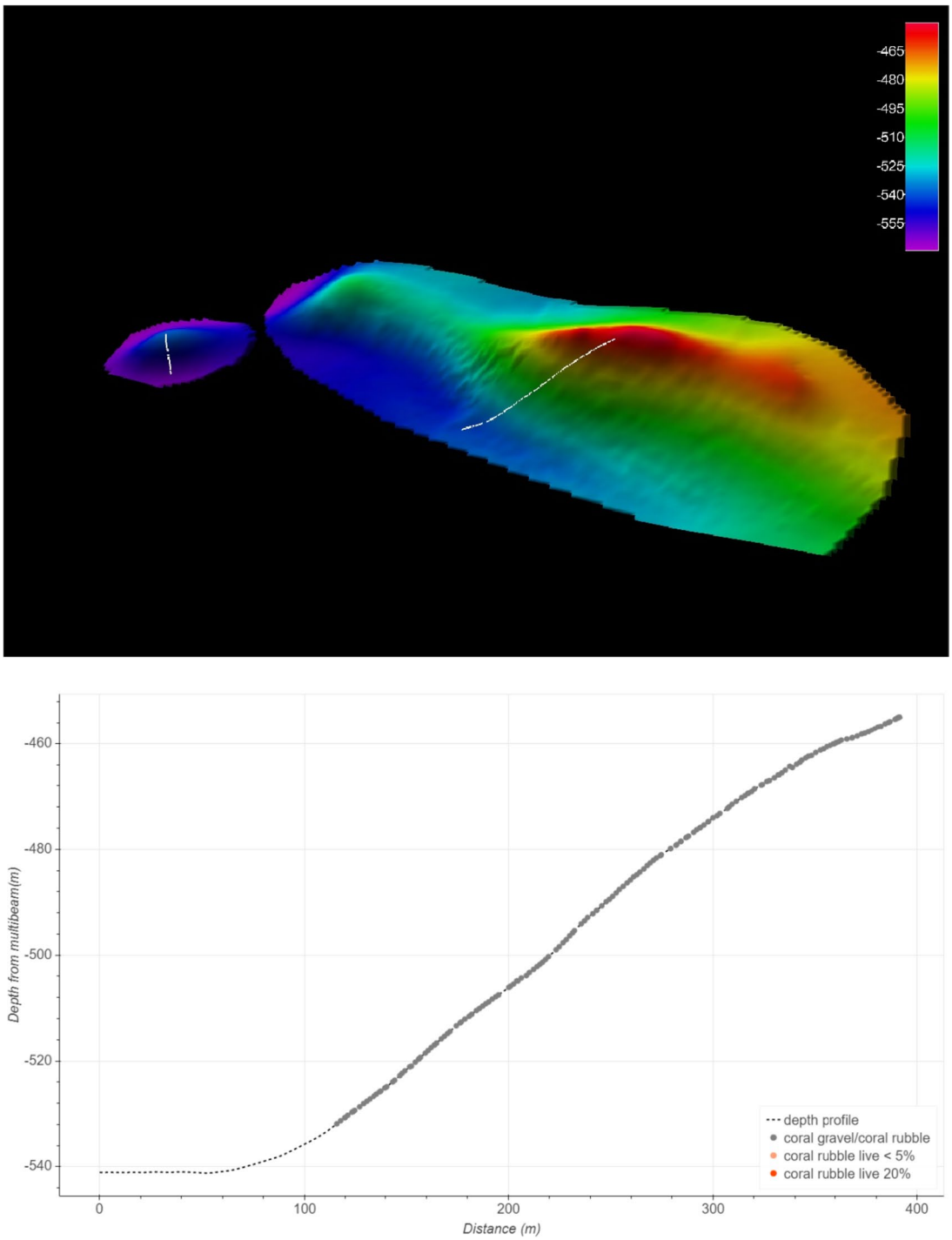

Fig. 7 In Area B the video transect surveys at station B6-3 covered two reefs. Above: the position of the transects is marked as a white line on a 3D bathymetry map with colors indicating depth, B6-3 to the right and B6-3B to the left. Below: The depth profile of transect B6-3 with the presence of Lophelia along the transect. Only a small colony of live coral was observed at B6-3, for details see Fig. 4

inorganic carbon (DIC) and nitrate (NO_3) increased (Figs. 9a–d; 10). This is likely caused by a gradually decreasing influence by the ENACW as it mixes with the MIW. In the upper 200 m, the warmest and most saline water was found mid-section at about 34.8 N, where the bottom shoals (Fig. 10a, b). At this point, the DO, DIC, ΩAr and NO_3 have lower concentrations than the surrounding water and further decreased with depth (Fig. 10c, e, f–h). The lowest DO, observed close to the seabed at the seabed at the northernmost station, was below 3.9

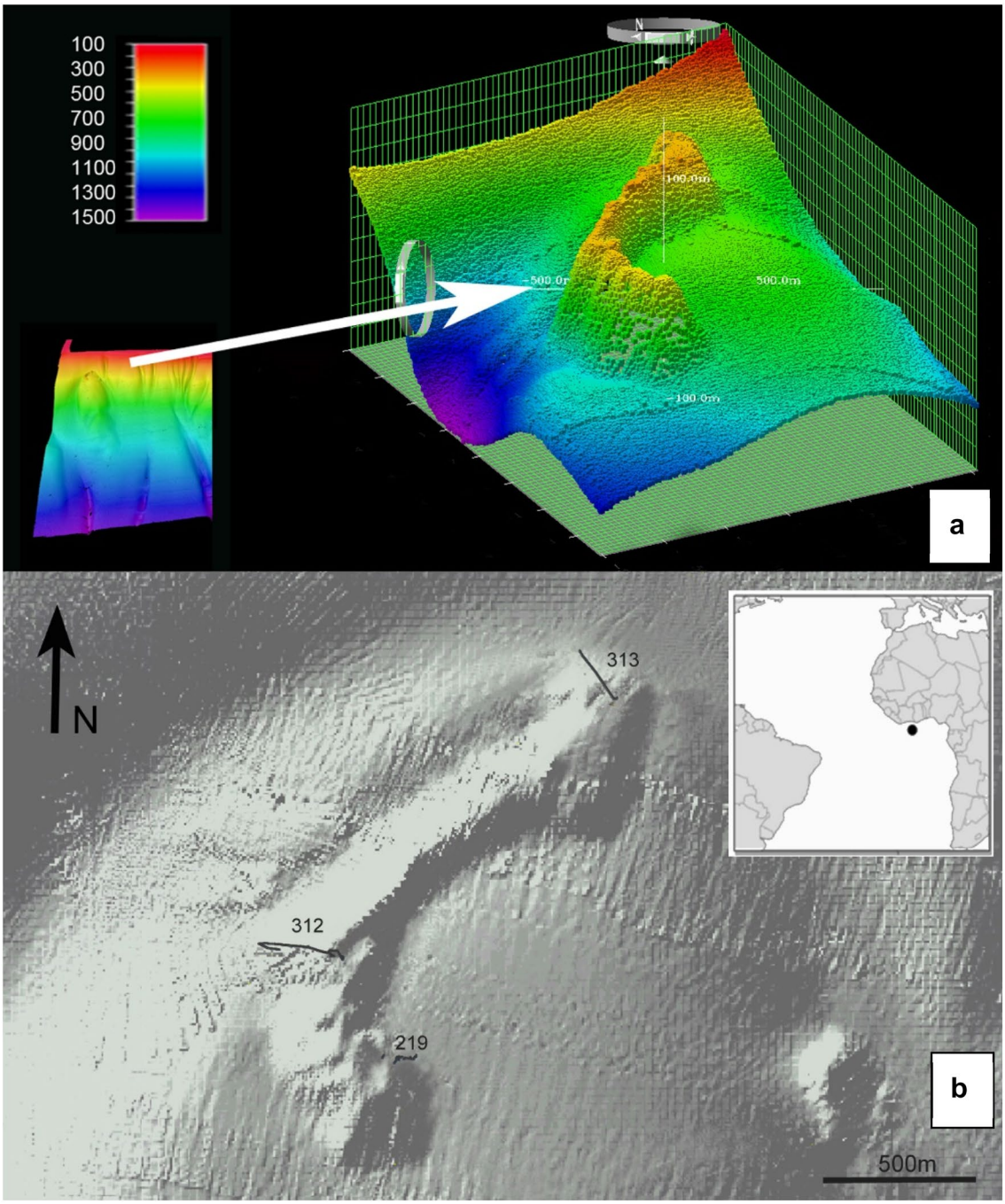

Fig. 8 The Lophelia reef on the Ghanian shelf in Area C. **a**. The position of the 70 m high and 1400 m long reef. The reef is curved and is located at 400 m depth on the continental slope off Ghana (colours indicates depth in meters). **b**. Shaded relief showing the position of three video transect surveys with station number

ml L^{-1}. Here, we also found the highest NO_3 concentrations (>17 µmol/L, Fig. 10h), suggesting the influence of MIW. DIC in the bottom is high over the whole section (>2170 µmol/kg) and increases towards the south to maximum values near 2200 µmol/kg (Fig. 10g), while pH and ΩAr decreased going south with minimum values of 7.93 and 1.65, respectively (Fig. 10e, f).

Area B

The surface layer in Area B is ventilated by the Mauritania Current and consists of relatively warm (15–22 °C) and salty (35.6-36.4 PSU) waters with a high DO concentration (4-6.8 ml L^{-1}) (Figs. 9e, f, 11a, b, f). Below the surface layer (~50m), the DO decreased considerably (minimum ~0.5 ml

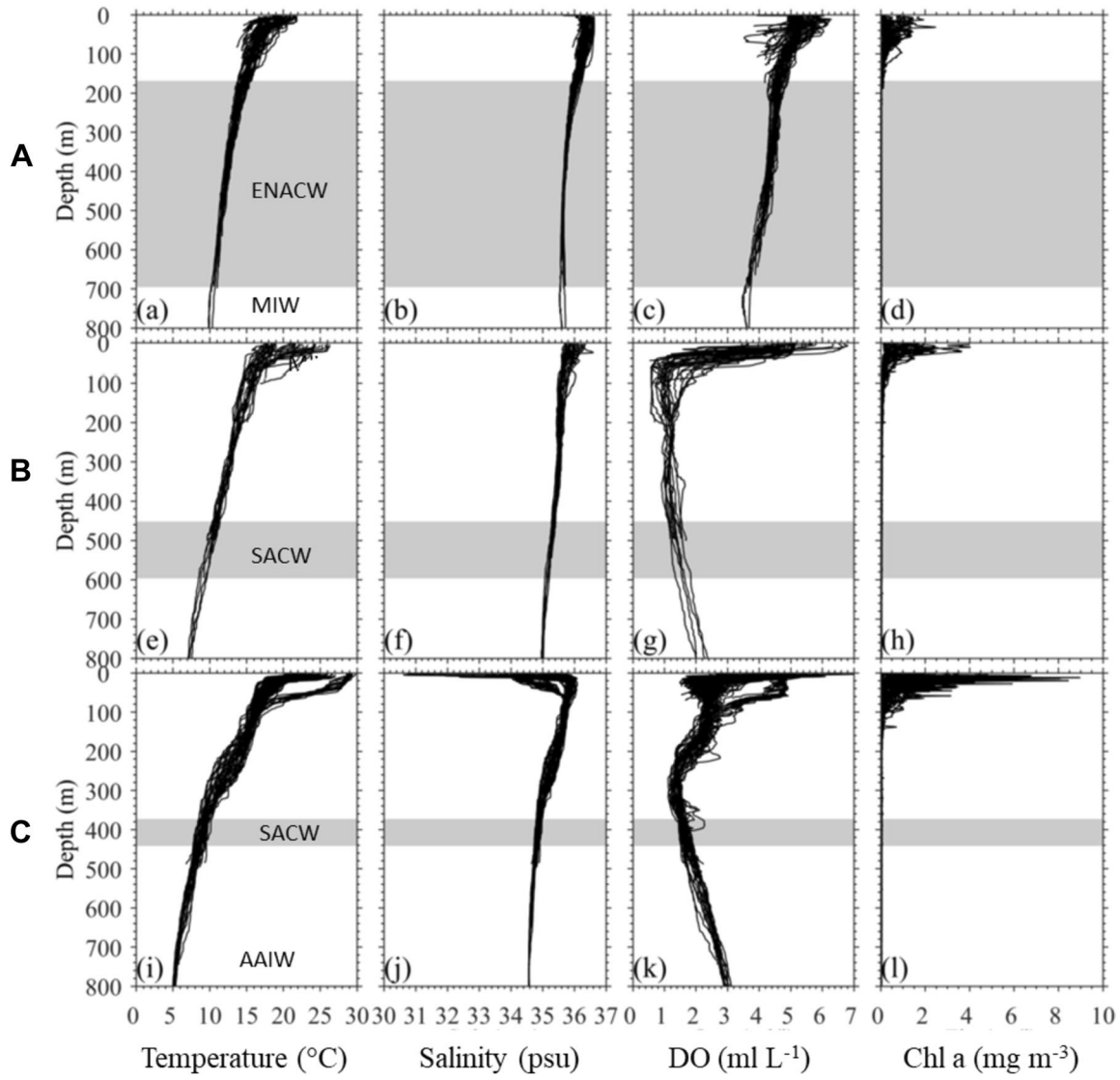

Fig. 9 Vertical profiles in the upper 800 m of, temperature (°C), practical salinity (Salinity, psu), dissolved oxygen (DO, ml L^{-1}), and chlorophyll a fluorescence (Chl a, mg m^{-3}) for the three areas A to C. The depth interval indicated with a gray shade is the depth zone where coral reefs were observed in the study areas

L^{-1}), as well as the temperature (<15°C). Salinity dropped slightly to ~35 PSU. A poorly ventilated upper thermocline was clearly visible between 450 and 600m depth (Figs. 9, 11a), that is occupied by relatively old South Atlantic Central Water (SACW). This is also the location of the observed coral reefs where the along-slope vertical distributions show relatively low DO (<1.5 ml L^{-1}) (Figs. 9, 11c). At the reef locations temperature is between 8 and 10 °C, the pH is very low, ΩAr values are near dissolution (~1), and coincide with high DIC (>2200 µmol/kg) and high NO_3 (Fig. 11e–h).

Area C

In Area C, the temperature and salinity distribution in the upper 800 m is presented in Figs. 9i, j and 12a, b. The upper 40 m of the water column from coast to offshore was relatively warm (>15°C), fresh, and salty (30.6-36.1 PSU) and DO concentrations ranging between 2 and 6 ml L^{-1} (Fig. 9k) and highest Chl a observed in all areas (Fig. 9l). A shallow thermocline at ~50 m separated cooler and low DO water from this upper layer. Below, the cooler (<15°C), salty (~35

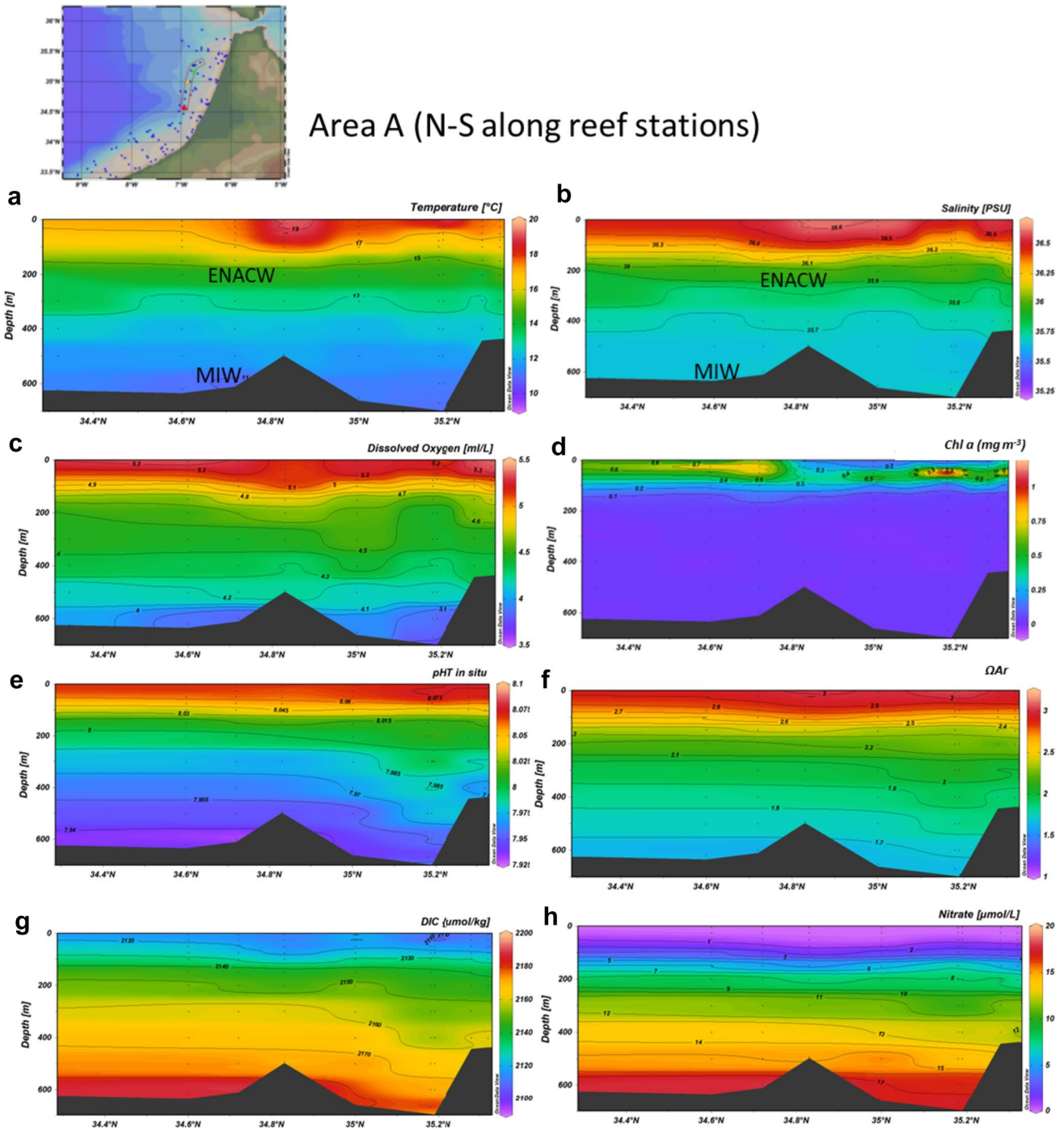

Fig. 10 Water column properties on reef sites from north to south in area A. **a**. Temperature (°C), **b**. Salinity (psu), **c**. Dissolved oxygen (DO, ml L^{-1}), **d**. chlorophyll a fluorescence (Chl a, mg m^{-3}), **e**. pH on total scale (pHT), **f**. aragonite saturation (ΩAr), **g**. total dissolved inorganic carbon (DIC, µmol kg^{-1}) and **h**. nitrate (µmol L^{-1})

PSU), and low DO waters (minimum ~1.1 ml L^{-1}) characteristic of the SACW dominates the water column. The SACW that is most visible between 200 and 600 m depth extends offshore and has low pH, and ΩAr values near or at dissolution concentration (<1), and high DIC and NO_3 concentrations (Fig. 12) that are especially visible on the slope between 300 and 400 m in 4.7 N and 4.8 N (Fig. 12f).

Interestingly, the observed coral reef occurs in the area with the lowest DO (Fig. 12d), pH (Fig. 12e), and ΩAr (Fig. 12f), and the highest DIC (Fig. 12g) (i.e., high CO_2,

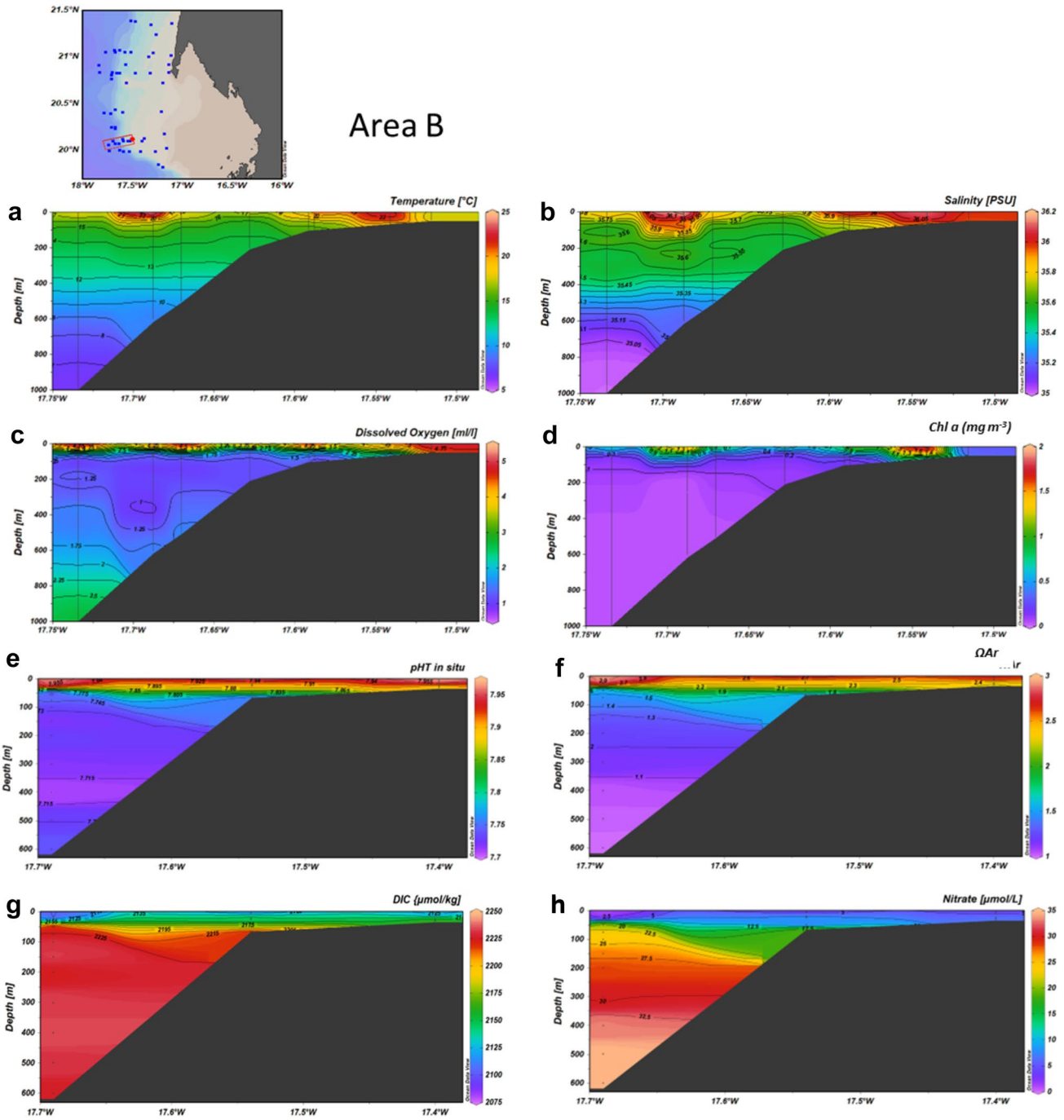

Fig. 11 Water column properties on reef sites from coast to offshore (east to west) in area B. **a**. temperature (°C), **b**. salinity (psu), **c**. dissolved oxygen (DO, ml L^{-1}) **d**. chlorophyll a fluorescence (Chl a, mg m^{-3}), **e**. pH on total scale (pHT), **f**. aragonite saturation (ΩAr), **g**. total dissolved inorganic carbon (DIC, µmol kg^{-1}) and **h**. nitrate (µmol L^{-1})

low pH) values (Fig. 9 i–l, grey shaded area). The water subsequently cools to <5°C from 600 m and below, a signature of the Antarctic Intermediate Water (AAIW). This water mass contains more DO and NO_3, and higher pH values than in SACW, but still, the ΩAr concentrations are at the minimum and are undersaturated (<1) (Fig. 12d).

Environmental parameters at coral sites

There is a clear contrast between the carbonate chemistry including the aragonite saturation in Area A and B. In general, the environmental settings in Area A appeared to be more favorable to aragonite-forming corals than Area B. In

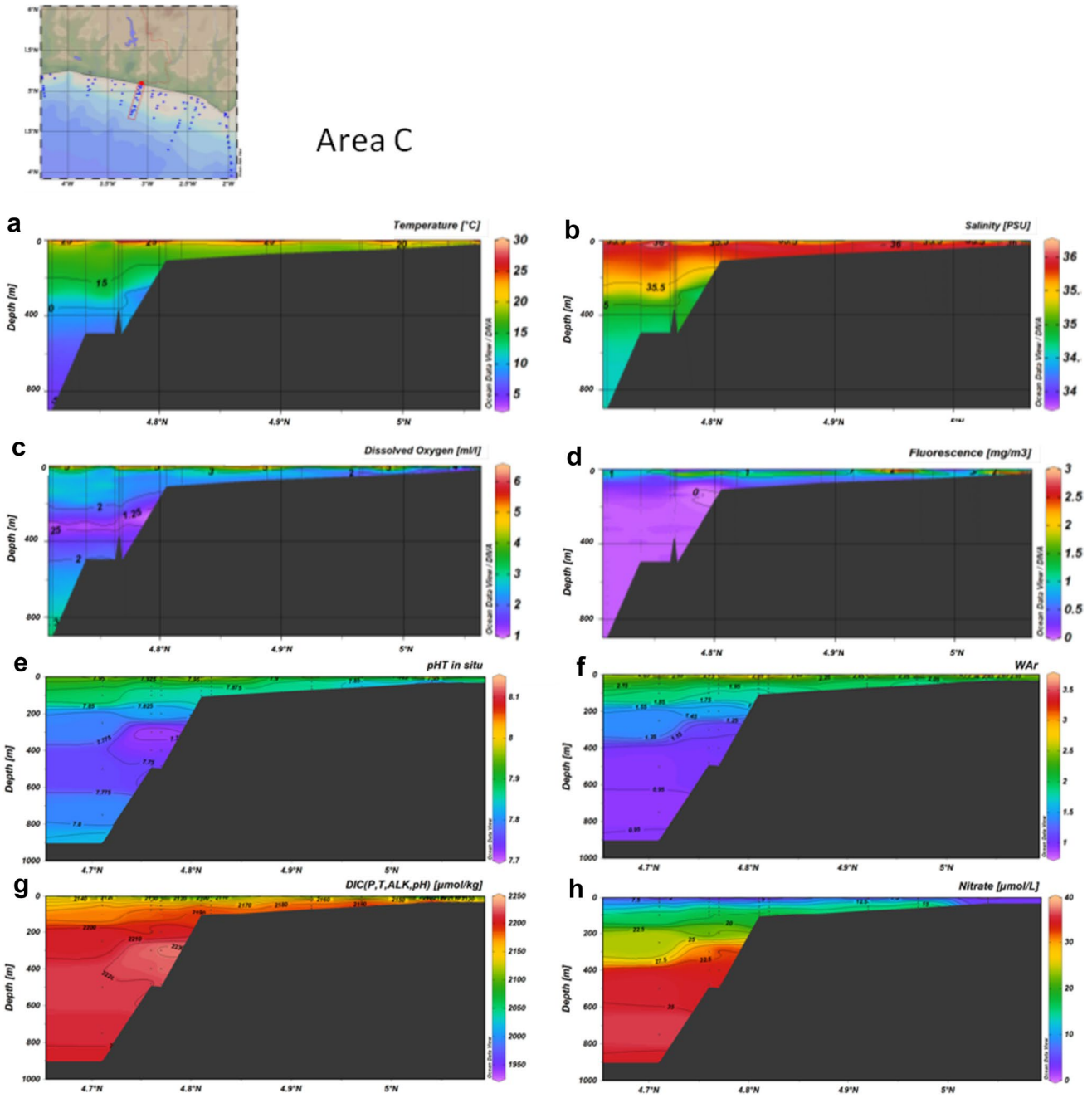

Fig. 12 Water column properties on reef sites from coast to offshore (east to west) in area C. **a**. temperature (°C), **b**. salinity (psu), **c**. dissolved oxygen (ml L^{-1}), **d**. chlorophyll a fluorescence (Chl a, mg m^{-3}), **e**. pHT, **f**. aragonite saturation (ΩAr), **g**. total dissolved inorganic carbon (DIC, µmol kg^{-1}) and **h**. nitrate (µmol L^{-1})

Area A the DO concentrations are relatively high (>3 ml L^{-1}) and DIC and CO_2 are at moderate concentrations and ΩAr is relatively high (Table 3). In Area B DO concentrations are low and between 1.30 and 1.65 ml L^{-1}, the DIC concentrations are among the highest in the study with a mean value of >2230 µmol/kg. Below 400m, ΩAr is undersaturated (<1) favoring the dissolution of the aragonite mineral (Fig. 16f). The mean values for the total alkalinity (AT) were similar in Area A and B, 2340 and 2320 µmol/kg, respectively. Since the mean values for AT are similar, we suggest that it is the higher DIC concentrations that result in the low ΩAr at Area B. This means that there are likely other causes for the non-living reefs on both sites than existing environmental conditions. This is also confirmed when comparing environmental conditions between B and C, where the environmental conditions are similar. In both areas,

healthy coral reef sites are located in the SACW, with the lowest DO concentrations, a ΩAr close to or at dissolution concentrations (ΩAr < 1), high DIC values (>2230 µmol/kg) and to AT (2330 µmol/kg, Table 3).

On a more local scale, the reefs with live *Lophelia* in Areas B and C were situated with their summit in the lower part of the oxygen minimum zone where the DO concentration start to increase with depth. Here the oxygen minimum zone stretched from 100 to 500 m with a slowly increasing DO concentration below 500 m (Figs. 9, 10, 11). The same feature was observed for the ΩAr which was lowest in the low oxygen zone, particularly evident in area B. The low DO concentration in this water mass coincides with a high concentration of DIC, nitrate and phosphate, suggesting a large influence from the decomposition of organic matter into CO_2 and nutrients (Figs. 9, 10, 11, 12).

In general, the oxygen minimum zone (OMZ) is related to the SACW which is an old water mass that makes little contact with the atmosphere, where accumulation and decomposition of organic matter result in low DO, high DIC and inorganic nutrients. During the composition of organic matter, oxygen is consumed and inorganic carbon (DIC, CO_2) and nutrients (e.g. nitrate) are produced leading to low DO and high DIC concentrations. As a consequence, the OMZ contains the lowest ΩAr concentrations and in Area C and B undersaturation with regard to aragonite is found below 400 m (Figs. 11f; 12f). The high particle load in these areas was confirmed by the video observations at the sites with live corals in Area B (reef B6–1 and B6-2) where large quantities of marine snow were observed (Supplementary information ESM 5). A reef positioned in the lower realm of the OMZ may benefit from plenty of food particles while at the same time avoiding the lower DO concentrations and higher temperatures at shallower depths. The Ghana reef in Area C was situated in a similar setting and in both Area B and C the healthy reefs were on the shelf slope break on the side of a canyon. It is also clear from ship and satellite data of Chl a as well as primary production (PP) data, that PP in upper water column was high at Area B and C (Figs. 11d, 12d, 14b, d). PP is seasonal and depends on the upwelling conditions along the coast (Fig. 13). Those sites are upwelling regions which are sites of high primary production, which may enhance the production in higher trophic concentrations and high vertical carbon transport to underlying water.

Primary production and potential food supply to corals based on satellite data

Area A

In Area A satellite data shows warm surface waters during July-September and a sea surface temperature anomaly (SSTA) exceeding 3°C (Fig. 13a), surface winds are mainly northerly (Fig. 13a) and surface currents predominantly westward (Fig. 13c). This indicates possible remote forcing of the surface currents. The surface waters are most productive during summer, and off the coast of Morocco, primary production (PP) can exceed 400 g C m^{-2} day^{-1} (Fig. 13c). During November-January the surface waters in Area A are cool with the winds becoming easterly and relatively weak offshore (Fig. 13b), meanwhile the surface currents are predominantly eastward, and the surface waters become less productive (Fig. 13d).

Area B

In Area B, the seasonal changes in surface oceanography are generally similar to those in Area A. The main difference between the two regions is that the winds and surface currents are stronger in Area B than in Area A leading to a higher primary production during summer (Fig. 13c).

Area C

In Area C the seasonal pattern of SSTA is opposite to patterns observed in Areas A and B. During boreal summer it experiences surface temperatures that could go 3 °C lower than the seasonal average (Fig. 13a). This low SSTA is primarily caused by wind-driven upwelling that brings cooler bottom waters to the surface and increases primary production especially off the coasts of Ivory Coast and Ghana (Fig. 13c) (Wiafe and Nyadjro 2015). Winds during this time are southwesterly (Fig. 13a) and the surface Guinea Current is eastward (Fig. 13c). However, during boreal winter, the surface waters in Area C are anomalously warm and the winds are northeasterly (Fig. 13b), while the Guinea Current is westward, and the region is less productive (Fig. 13d).

Discussion

Contrasting reef conditions and vulnerability

To obtain knowledge on the physiological ranges and adaptive capacity of *Lophelia* reefs we compared the health status and environmental conditions of the coral reef sites on the Mauritania-Morocco and Ghana/Ivory coast and shelf/slope with information from other known reefs. In table 3, the health status of coral reefs from our study is listed together with the ocean chemistry information from reef areas in other regions.

Norway is one of the North Atlantic countries with the most occurrences of *Lophelia* reefs. In Fig. 14 we present the relation between coral health, temperature, and DO

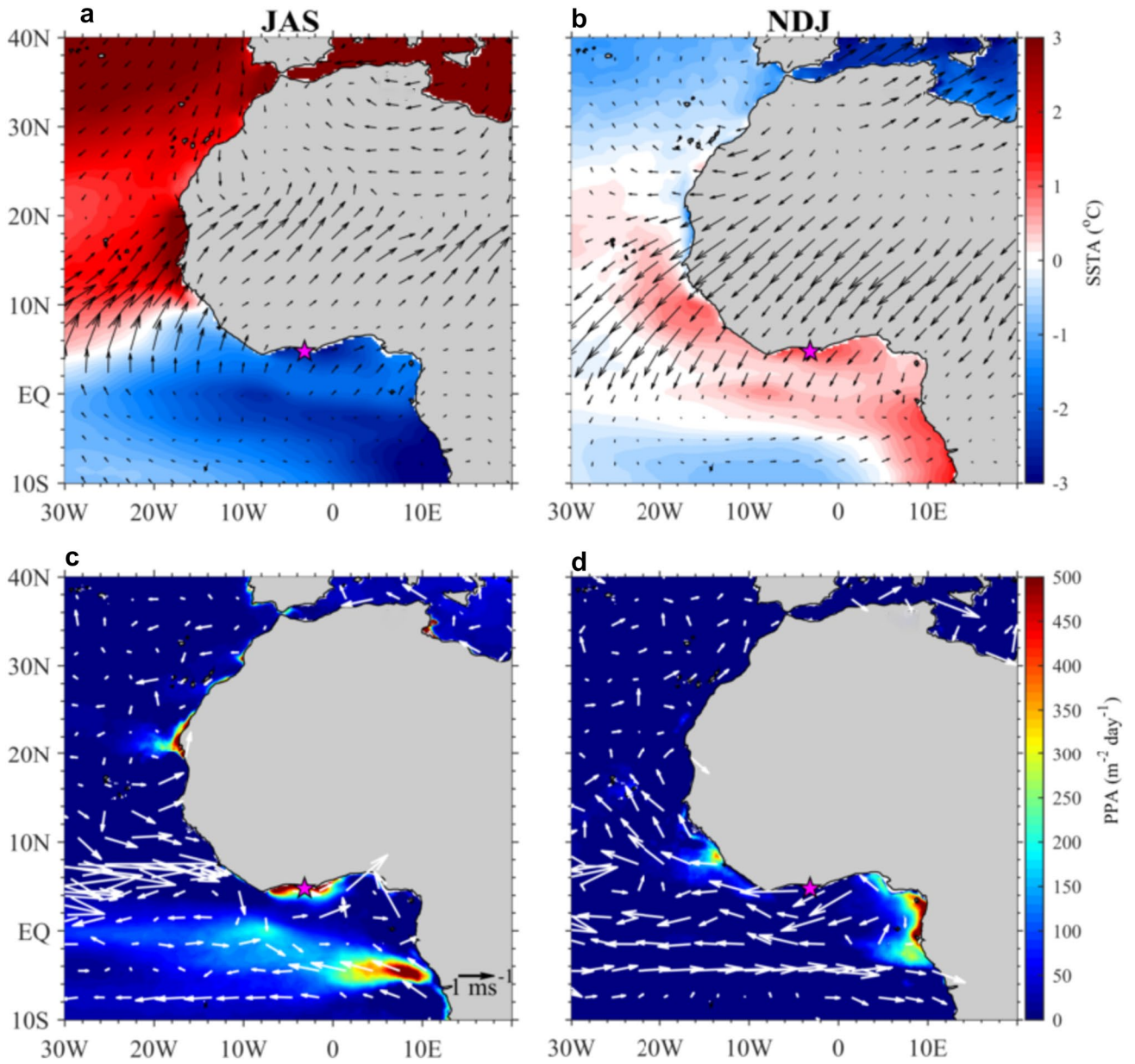

Fig. 13 **a**. and **b**. Anomalies for composite means of sea surface temperature (°C; color shading) and surface winds (ms^{-1}; vectors) for July–September (JAS) and November–January (NDJ). **c** and **d**. Primary production (gCm^{-2} day-1; color shading) and surface currents (ms^{-1}; vectors) for the same seasons. Pink stars mark the location of the reefs on the coast off Ghana/ Ivory Coast

concentration. Norwegian reefs are in areas with DIC and AT conditions resulting in relatively high ΩAr between 1.7 and 2 (Table 3), and DO of about 5 ml L^{-1} (Fig. 14). The largest contrast between Norwegian and West African reefs concerning the carbonate chemistry is observed in the DIC and ΩAr. In Areas B and C, the DIC mean values reached 2260 µmol/kg, nearly 100 µmolkg^{-1}) higher than is considered to be the threshold for healthy reefs (Flögel et al. 2014; DIC of <2170 µmol/kg). High DIC values (2200 µmol/kg) were found on wall reefs in Norwegian fjords and are considered to be sentinels for future climate change (Juva et al., 2021). This suggests that the reef in Ghana may have some adaptive capacity, which has also been indicated for *Lophelia* reefs in the Mediterranean (Maier et al. 2013).

Before the present study, reefs off Mauritania were reported to be in a dormant state with only sporadic occurrences of live corals and at oxygen concentrations of 1.1–1.4 mL L^{-1} (Wienberg et al. 2018), which are similar concentrations to our study. The few live colonies present in the area were viewed as part of a re-colonization of old and long-dead coral mounds. Based on paleo studies,

Table 3 Health status and depth of coral reefs listed together with the mean for ocean chemistry measurements conducted at depth relevant for reef sites in Area A, B, and C (data sources are listed in Supplementary information ESM 1)

Area/Station	Reef status	Reef depth	Depth m	Temp. °C	Oxygen ml/l	ΩAr	pHT	AT µmol/kg	DIC µmol/kg	pCO2 µatm	NO3 µmol/l	PO4 µmol/l
Area A												
5–7	Dead	700–692	679	11.08	3.87	1.63	7.938	2340	2175	496	17.09	1.02
			696	11.10	3.89	1.66	7.940	2346	2182	497	17.52	1.05
5–8	Dead	661–574	574	11.34	4.01	1.66	7.943	2346	2174	487	15.53	0.96
			675	11.49	4.09	1.75	7.954	2348	2181	492	16.99	
5–9	Dead	241–213	169	15.34	4.67	2.39	8.016	2373	2148	432	5.55	0.42
			245	15.47	4.71	2.40	8.019	2378	2151	436	5.77	0.42
Area B												
6–1B	Healthy	562–538	486	9.66	1.48							
	Poor	597–559	597	9.96	1.52							
6–2	Poor	536–525	520	9.95	1.38							
			581	10.45	1.48							
6–3	Poor	515–469	452–542	9.68	1.31	1.04	7.740	2317	2236	812	30.88	1.81
6–3B	Dead	577–490	533–551	10.53	1.51	1.12	7.746	2324	2236	841	32.20	1.87
6–4	Dead	585–505	503	10.30	1.34							
			575	11.02	1.46							
6–5	Dead	577–490	489	10.12	1.64	1.10	7.761	2321	2230	781	28.41	1.69
			583	10.20	1.65	1.20	7.764	2328	2232	801	30.79	1.89
Area C												
219	Poor	403–485	385	9.54	1.47	1.00	7.724	2305	2230	830	33.34	2.08
			423	9.76	1.53	1.04	7.736	2313	2238	879	34.08	2.10
312	Healthy	428–374	375	9.47	1.47	1.00	7.724	2305	2230	830	33.34	2.08
			442	9.76	1.55	1.04	7.736	2313	2238	879	34.08	2.10
313	Healthy	375–373	373	9.70	1.47	1.00	7.724	2305	2230	830	33.34	2.08
			402	9.76	1.48	1.04	7.736	2313	2238	879	34.08	2.10
Norway												
Hola (1)	Healthy	260		6.70		1.72	8.01	2314	2135	364	3.77	0.48
				8.18		1.91	8.07	2332	2162	419	11.69	0.73
Wall (2)	Healthy	80 –220		7.51	4.96	1.5	7.944	2300	2136	374	8.64	0.67
				12.2	5.81	1.98	8.063	2330	2187	501	11.61	0.96
Banks (2)	Healthy	190–220		7.53	5.07	1.56	7.968	2317	2135	356	10.40	0.69
				8.35	5.75	2.01	8.081	2343	2192	506	11.37	0.89
Mauritania (3)	Healthy	596–560		10.0–12.0	1.1–1.4							
Namibia (4)	Dead	260–160		11.8–13.2	0–0.15		8.010					
Angola (4)	Healthy	473–331		7.8–11.1	0.6–1.1		8.120					
	Poor	260–250		11.1–14.1	0.7–0.9							
Gulf of Mexico (5)	Healthy	600–500		6.6–11.6	2.7–2.8							

Reef status: "Dead" no observations of live colonies, "Poor" only few live colonies. and "Healthy" larger areas with live colonies. For comparison the lower part of the table includes information from *Lophelia* reefs in Norway, other regions off west Africa and the Gulf of Mexico with reported reef status and ocean chemistry measurements from literature. Sources are: (1) Järnegren and Kutti (2014), (2) Juva et al. (2021), (3) Phaeton report (2012), (4) Hanz et al. (2019), (5) Matos (2017)

Wienberg et al. (2018) and Tamborrino et al. (2019) hypothesized that regional changes in water column structure during the last ~20,000 years had caused a collapse of these *L. pertusa* dominated ecosystems due to decreasing DO concentrations, an explanation that was supported by Portilho-Ramos et al. (2022).

This contrasts with our documentation of healthy reefs occurring under hypoxic conditions off Mauritania which agrees with reports from African reefs by Buhl-Mortensen et al (2017) and Hanz et al. (2019). The latter found that *L.*

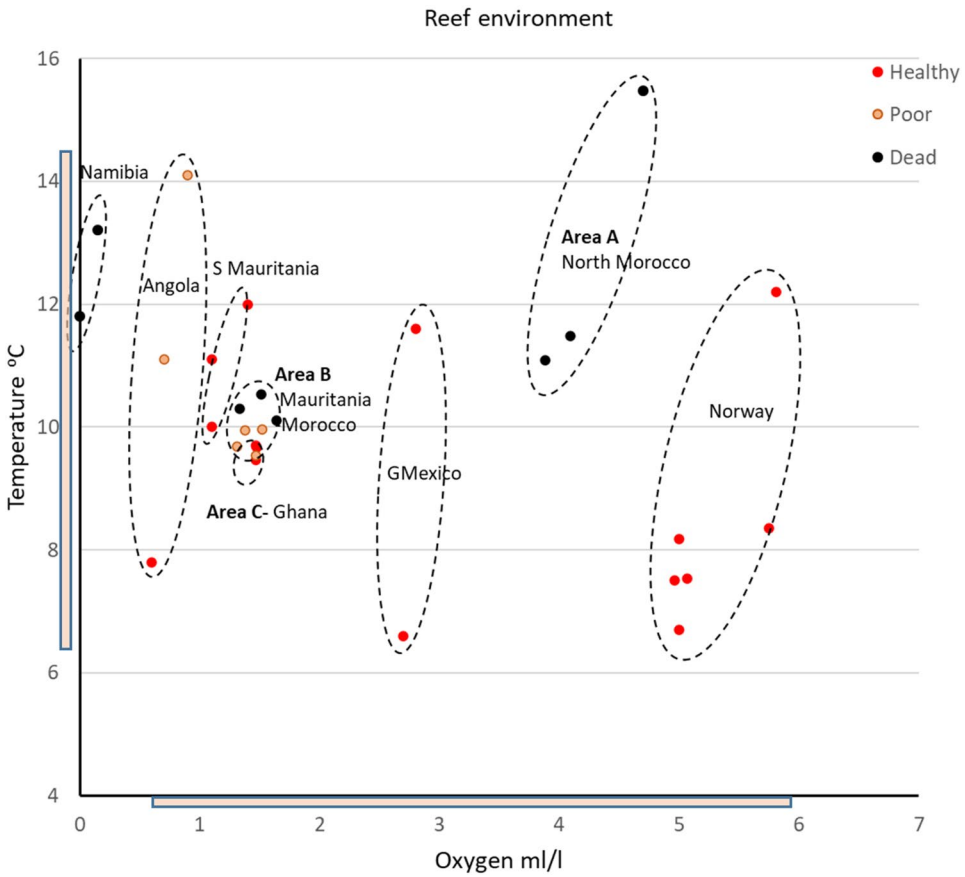

Fig. 14 Plot of the temperature and oxygen setting in Lophelia reef areas with health status indicated by symbols. Red circle: healthy reef with large areas having a dense cover of live colonies. Pink circle: poor reef with only a few occurrences of live colonies. Black circle: dead reef with only the presence of coral skeleton. Pink bar along the axis indicates range for the occurrence of live Lophelia. Reefs are encircled in accordance with geographic area. Background data is provided in Table 3

pertusa could thrive in hypoxic and rather warm waters in the NE Atlantic off Angola. Hebbeln et al. (2020) stated that reefs appear to thrive at DO concentrations of 1 ml L^{-1} and at temperatures up to 14.2 °C and the authors speculate that the negative effects of hypoxia and high temperature could be compensated for by enhanced food supply. This theory seems to be at odds with the general observation that increased feeding will increase respiration rate (Maier et al. 2013) and thus the oxygen demand. In addition, an increased load of organic particles will demand more mucus production to clean the coral which in turn would increase respiration and oxygen demand (Buhl-Mortensen et al. 2015a, b).

The relationship between reef health and environmental conditions (Fig. 14) indicates that the tolerance window for hypoxia is larger than for temperature. This supports the view that *L. pertusa* as a species appears to have a high oxygen tolerance, but individual populations could have limited adaptive capabilities to cope with reductions (Dodds et al. 2007; Lunden et al. 2013). The tolerance to hypoxia could be related to the relatively low respiration rate of cold water Scleractinia (Buhl-Mortensen et al. 2007, Maier 2013). Maier et al. (2013) and Hebbeln (2020) suggest that local adaptation can affect tolerance to environmental stressors and highlights the need to compare reefs in contrasting settings.

Environmental conditions and age and growth of reefs

Both the Mauritanian and Ghanaian reefs are of substantial size and occurs in a region where the conditions during the last ice age allowed for continued growth. Reefs off Norway have been aged using radiocarbon and Uranium/Thorium techniques (Mikkelsen et al.1982; Mortensen 2000; Rokoengen and Østmo 1985), estimating a maximum age of around 9000 years. The vertical extension of a 30 m high and 9000-year-old reef indicates a reef growth of 3.3 mm $year^{-1}$. Applying this reef growth rate to the African reefs, heights of 60 to 70 m, indicates continuous growth for at least 20,000 years. This is in line with the U/Th-dating of deep-water corals from seamounts off NW-Africa by Schröder-Ritzrau et al. (2005) which showed that the corals have had continuous growth over the last 53,000 years. This does not support the hypothesis that live colonies in the region represent a re-colonization of old and dead reefs proposed by Wienberg et al. (2018), Tamborrino et al. (2019) and Portilho-Ramos et al. (2022). On the Norwegian shelf, the main temperatures in areas where thriving old reefs are located range from 4 to 12 °C. The temperature range of

8.5–9 °C recorded at the African reef sites examined in this study falls within this established range. Therefore, disparities in temperature are unlikely to account for the observed variations in size. Furthermore, reefs in both areas occur in highly productive upwelling settings with a good food supply. There is, however, a possibility that the reef growth was interrupted at some stage during the Holocene transgression or the Holocene itself. Ayers and Pilkey (1981) have dated some coral samples from the Florida–Hatteras slope and inner Blake Plateau, in the Western Atlantic. Their dead coral samples ranged in age from 5000 to 44,000 years old. The much younger age of Norwegian reefs reflects the strong glacial influence (Mortensen 2000). Verification of reef age will require the ageing of skeleton sampled by coring to the base of the reef. Cores have been collected from reef remnants in other areas of Africa but results on age have to our knowledge not yet been published (Westphal et al. 2012 unpublished data).

Conclusions

Based on many studies from the North Atlantic the assumed lower limit of oxygen tolerance of *L. pertusa* ranges around a DO concentration of 2–3.7 ml L^{-1}. However, the first large and healthy reef off Atlantic Africa was found off Ghana in the OMZ zone (Buhl-Mortensen et al. 2017). Our study has shown that large and old thriving reefs occur off Africa in areas with low oxygen concentrations. Clearly, this species has a broad tolerance for oxygen concentrations at least down to 1 ml L^{-1}, altering our view on oxygen demand for *L. pertusa* .

The African reefs are much older than the northern counterpart which clearly shows that low DO consentration, pH, and low ΩAr are not hindering rich and healthy *Lophelia* reefs, this is in line with the observations by Maier et al. (2013) who found that *Lophelia* reefs in the Mediterranean are not affected by or may be adapted to corrosive aragonite conditions. However, studies show that calcifying organisms can calcify at corrosive conditions but to an energetic cost (Spalding et al. 2017).

The reefs in the OMZ co-occur with a rich load of organic particles and are probably more than double the age of northern reefs. The OMZ reefs will trap a lot of sediment during their growth. Likely both growth and aging patterns differ from the northern reefs as do tolerances to environmental stressors: e.g., lower oxygen, pH, ΩAr, industrial activities resulting in physical damage and increased silting. Even though climatic changes causing a decrease in oxygenation might not be a serious threat to *Lophelia* reefs in general, in already hypoxic settings this might be different. Even if smaller decreases in DO alone might not pose a serious threat to *Lophelia* reefs, they must be considered in concert with other changing environmental parameters that might form additional stressors such as increased temperature and physical pressure from silting and crushing related to industrial activities such as fisheries. The dead or almost dead reefs we observed in Area B near an old healthy and large reef had signs of physical damage that can be attributed to trawling.

Our findings highlight the importance of continued studies of *Lophelia* reefs in contrasting environmental conditions to improve our understanding of their resilience and adaptation potential in relation to climate change, ocean acidification, and other stressors.

Acknowledgements This paper uses data collected through scientific surveys with the research vessel Dr. Fridtjof Nansen as part of the collaboration between the Food and Agriculture Organization of the United Nations (FAO) on behalf of the EAF-Nansen Programme. The EAF-Nansen Programme is a partnership between the FAO, the Norwegian Agency for Development Cooperation (Norad), and the Institute of Marine Research (IMR) in Norway for sustainable management of the fisheries in partner countries and regions. We are grateful to all cruises and their participants for their help and support during the data collection.

Funding Open access funding provided by Institute Of Marine Research. All authors certify that they have no affiliations with or involvement in any organization or entity with any financial interest or non-financial interest in the subject matter or materials discussed in this manuscript. The authors have no financial or proprietary interests in any material discussed in this article.

Data availability Data is available upon request.

Declarations

Conflict of interest The authors have no relevant financial or non-financial interests to disclose. The authors have no competing interests to declare that are relevant to the content of this article. No experimental use of organisms was part of this study.

References

Addamo AM, Vertino A, Stolarski J, García-Jiménez R, Taviani M, Machordom A (2016) Merging scleractinian genera: the overwhelming genetic similarity between solitary *Desmophyllum*

and colonial *Lophelia*. BMC Evolut Biol 16(1):118. https://doi.org/10.1186/s12862-016-0654-8

Agudo-Bravo, LM, Mangas J (2015) Main geomorphologic features in the Canary Current LargeMarine Ecosystem. (eds) Valdés L, Déniz-González I, Oceanographic and biological features in the Canary Current Large Marine Ecosystem. IOC-UNESCO, Paris. IOC Technical Series 115:23-38. http://hdl.handle.net/1834/9174.

Arístegui J, Barton ED, Álvarez-Salgado XA, Santos MP, Figueira FG et al (2009) Sub-regional ecosystem variability in the Canary Current upwelling. Progress Oceanogr 83(1–4):33–48. https://doi.org/10.1016/j.pocean.2009.07.031

Ayers MW, Pilkey OH (1981) Pistoncores and surficial sediment investigations of the Florida-Hatteras slope and inner Blake Plateau. In: Popenoe P (ed) Environmental geologic studies on the southeastern Atlantic outer continental shelf. USGS Open File Report, USA, p 5

Bakun A (1978) Guinea Current Upwelling. Nature 271:147–150

Bakun A (1990) Global climate change and intensification of coastal ocean upwelling. Science 247(4939):198–201. https://doi.org/10.1126/science.247.4939.198

Barton ED, Field DB, Roy C (2013) Canary current upwelling: More or less? Progress Oceanogr 116:167–178. https://doi.org/10.1016/j.pocean.2013.07.007

Benazzouz A, Demarcq H, González-Nuevo G (2015) Recent changes and trends of the upwelling intensity in the Canary Current Large Marine Ecosystem. In: Valdés L, Déniz-González I (eds) Oceanographic and biological features in the Canary Current Large Marine Ecosystem. IOC Technical Series, Mexico, pp 321–330

Binet D (1997) Climate and pelagic fisheries in the Canary and Guinea currents 1964–1993: The role of Trade Winds and the Southern Oscillation. Oceanol Acta 20:177–190

Bonjean F, Lagerloef GSE (2002) Diagnostic model and analysis of the surface currents in the Tropical Pacific Ocean. J Phys Oceanogr 32(10):2938–2954

Buhl-Mortensen L, Mortensen PB, Armsworthy S, Jackson DL (2007) Field observations of Flabellum spp. and laboratory study the behavior and respiration of Flabellum alabastrum. Bull Mar Sci 81(3):543–552

Buhl-Mortensen L, Vanreusel A, Gooday AJ, Levin LA, Priede IG, Buhl-Mortensen P, Gheerardyn H, King NJ, Raes M (2010) Biological structures as a source of habitat heterogeneity and biodiversity on the deep ocean margins. Mar Ecol 31(1):21–50

Buhl-Mortensen L, Olafsdottir SH, Buhl-Mortensen P, Burgos JM, Ragnarsson SA (2015) Distribution of nine cold-water coral species (Scleractinia and Gorgonacea) in the cold temperate North Atlantic in light of bathymetry and hydrography. Hydrobiologia 759:39–61

Buhl-Mortensen P, Tenningen E, Tysseland ABS (2015) Effects of water flow and drilling waste exposure on polyp behaviour of *Lophelia pertusa*. Mar Biol Res 11:725–737

Buhl-Mortensen P, Buhl-Mortensen L, Purser A (2016) Trophic Ecology and Habitat Provision in Cold-Water Coral Ecosystems. In Marine Animal Forests. Springer International Publishing, Cham, pp 1–6

Buhl-Mortensen L, Serigstad B, Buhl-Mortensen P, Olsen MN, Ostrowski M, Błażewicz-Paszkowycz M, Appoh E (2017) Structure and megafaunal community of a large *Lophelia* reef on the Ivorian-Ghanaian margin (the Gulf of Guinea). Deep Sea Res 137:148–156. https://doi.org/10.1016/j.dsr2.2016.06.007

Chierici M, Drange H, Anderson LG, Johannessen T (1999) Inorganic carbon fluxes through the boundaries of the Greenland Sea Basin based on in situ observations and water transport estimates. J Mar Syst 22(4):295–309. https://doi.org/10.1016/S0924-7963(99)00069-X

Clayton TD, Byrne RH (1993) Spectrophotometric seawater pH measurements: total hydrogen ion concentration scale calibration of m-cresol purple and at-sea results. Deep-Sea Res I 40(10):2115–2129

Colman JG, Gordon DM, Lane AP, Forde MJ, Fitzpatrick JJ (2005) Carbonate mounds off Mauritania, Northwest Africa: status of deep-water corals and implications for management of fishing and oil exploration activities. In: Freiwald A, Roberts JM (eds) Cold-Water Corals and Ecosystems, Erlangen Earth Conference Series. Springer, Berlin, Heidelberg. https://doi.org/10.1007/3-540-27673-4_21

Cudjoe JE, Khan MH (1972) A preliminary report on the geology of the continental shelf of Ghana. Fish Res Unit, TEMA, Ghana, Mar Fish Res Repts 204:22

Davies AJ, Guinotte JM (2011) Global Habitat Suitability for Framework-Forming Cold-Water Corals. PLoS One 6(4):e18483. https://doi.org/10.1371/journal.pone.0018483

DeCastro M, Gómez-Gesteira M, Costoya X, Santos F (2014) Upwelling influence on the number of extreme hot SST days along the Canary upwelling ecosystem. J Geophys Res Oceans 119(5):3029–3040. https://doi.org/10.1002/2013JC009745

Dickson AG (1990) Standard potential of the (AgCl(s)11/2H2 (g) 5Ag(s)1HCl(aq)) cell and the dissociation constant of bisulfate ion in synthetic sea water from 273.15 to 318.15 K. J Chem Thermodyn 22:113–127. https://doi.org/10.1016/0021-9614(90)90074-z

Dickson AG, Millero FJ (1987) A comparison of the equilibrium constants for the dissociation of carbonic acid in seawater media. Deep Sea Res Part A 34:1733–1743. https://doi.org/10.1016/0198-0149(87)90021-5

Dickson AG, Sabine CL, Christian JR (2007) Guide to best practices for ocean CO_2 measurement. Sidney, British Columbia, North Pacific Marine Science Organization PICES Special Publication 3, IOCCP Report 8. p 19

Dodds LA, Roberts JM, Taylor AC, Marubini F (2007) Metabolic tolerance of the cold-water coral *Lophelia pertusa* (Scleractinia) to temperature and dissolved oxygen change. J Exp Mar Biol Ecol 349(2):205–214

Dullo W, Chr Flögel S, Rüggeberg A (2008) Cold-water coral growth in relation to the hydrography of the Celtic and Nordic European continental margin. Mar Ecol Progress Ser 371:165–175

Emery WJ (2001) Water types and water masses. Encycl Ocean Sci. https://doi.org/10.1006/rwos.2001.0108

Fischer JG (2008) Circulation in the Gulf of Guinea. Thesis Mathematisch-Naturwissenschaftliche Fakultät der Christian-Albrechts-Universität zu Kiel 73pp. https://www.researchgate.net/publication/291351905.

Flögel S, Dullo W-C, Pfannkuche O, Kirikoulakis K, Rüggeberg A (2014) Geochemical and physical constraints for the occurrence of living cold-water corals. Deep Sea Res Part II: Topical Stud Oceanogr 99:19–26. https://doi.org/10.1016/j.dsr2.2013.06.006

Frederiksen R, Jensen A, Westerberg H (1992) The distribution of the scleractinian coral *Lophelia pertusa* around the Faroe Islands and the relation to internal mixing. Sarsia 77:157–171

Freiwald A, Wilson JB, Henrich R (1999) Grounding Pleistocene icebergs shape recent cold-water coral reefs. Sed Geol 125:1–8

Gibbons W, Moreno T (2002) The Geology of Spain. Geological Society of London, London, p 664

Grasshoff K, Ehrhardt M, Kremling K (1983) Methods of seawater analysis. Verlag Chem., Weinheim, 419 pp

Gundersen K, Møgster JS, Lien V, Lunde LF, Arnesen H, Olsen AK, Morvik A, Yamakawa A, Jakobsson Ø, Broms CT (2022) Nutrient Biogeochemistry in the Nordic Seas (Norwegian, Greenland and Iceland Seas). Sci Data. https://doi.org/10.21335/NMDC-482758181

Hanz U, Wienberg C, Hebbeln D, Duineveld G, Lavaleye M et al (2019) Environmental factors influencing benthic communities in the oxygen minimum zones on the Angolan and Namibian margins. Biogeosciences 16:4337–4356. https://doi.org/10.5194/bg-16-4337-2019

Hebbeln D, Wienberg C, Dullo WC et al (2020) Cold-water coral reefs thriving under hypoxia. Coral Reefs 39:853–859. https://doi.org/10.1007/s00338-020-01934-6

Henin C, Hisard P, Piton B (1986) Observations hydrologiques dans l'ocean Atlantique Equatorial. ORSTOM. Focal, Paris, pp 1–191

Ingham MC (1970) Coastal upwelling in the northwestern gulf of Guinea. Bull Mar Sci 20:1–34

IPCC (2019) Climate Change and Land: an IPCC special report on climate change, desertification, land degradation, sustainable land management, food security, and greenhouse gas fluxes in terrestrial ecosystems. In: Shukla PR, Skea J, Calvo Buendia E, Masson-Delmotte V, Pörtner H-O, et al. (eds) 864 pp

Juva K, Kutti T, Chierici M, DulloW-C Flögel S (2021) Cold-Water Coral Reefs in the Langenuen Fjord, Southwestern Norway—A Window into Future Environmental Change. Oceans 2:583–610. https://doi.org/10.3390/oceans2030033

Kifani S, Quansah E, Masski H, Houssa R, Hilmi K (2018) Climate change impacts, vulnerabilities and adaptations: Eastern Central Atlantic marine fisheries. Impacts of climate change on fisheries and aquaculture Synthesis of current knowledge, adaptation and mitigation options. FAO Fish Aquac Tech Paper 627:159–183

Järnegren & Kutti (2014) *Lophelia pertusa* in Norwegian waters. What have we learned since 2008? NINA-Report pp 1028 40

Lima FP, Wethey DS (2012) Three decades of high-resolution coastal sea surface temperatures reveal more than warming. Nat Commun 3:704. https://doi.org/10.1038/ncomms1713

Longhurst AR (1962) A review of the Oceanography of the Gulf of Guinea. Bull Inst Afr Noire 24:633–663

Lunden J, Georgian S, Cordes E (2013) Aragonite saturation states at cold-water coral reefs structured by *Lophelia pertusa* in the Northern Gulf of Mexico. Limnol Oceanogr 58(1):354–362. https://doi.org/10.4319/lo.2013.58.1.0354

Ly CK (1980) The Role of the Akosombo Dam on the Volta River in Causing Coastal Erosion in Central and Eastern Ghana (West Africa). Mar Geol 37:323–332

Maier C, Bils F, Weinbauer MG, Watremez P, Peck MA, Gattuso J-P (2013) Respiration of Mediterranean cold-water corals is not affected by ocean acidification as projected for the end of the century. Biogeosci Discuss 10:7617–7640

Matos L (2017) Temporal distribution of cold-water corals in the northwest Atlantic through the Late Quaternary: footprint of intermediate water mass circulation. Dissertation for obtaining the Doctoral degree in natural sciences in the Department of Geosciences. University of Bremen, Bremen p, p 144

Mears CA, Scott J, Wentz FJ, Ricciardulli L, Leidner SM, Hoffman R, Atlas R (2019) A Near-Real-Time Version of the Cross-Calibrated Multiplatform (CCMP) Ocean Surface Wind Velocity Data Set. J Geophys Res Oceans 124:6997–7010

Mehrbach C, Culberson CH, Hawley JE, Pytkowicz RM (1973) Measurement of the apparent dissociation constants of carbonic acid in seawater at atmospheric pressure. Limnol Oceanogr 18:897–907. https://doi.org/10.4319/lo.1973.18.6.0897

Mikkelsen N, Erlenkeuser H, Killingley JS, Berger WH (1982) Norwegian corals: radiocarbon and stable isotopes in *Lophelia pertusa*. Boreas 11(2):163–171. https://doi.org/10.1111/j.1502-3885.1982.tb00534.x

Mittelstaedt E (1991) The ocean boundary along the northwest African coast. Circulation and oceanographic properties at the sea surface. Progress Oceanogr 26:307–355

Mortensen PB, Hovland M, Brattegard T, Farestveit R (1995) Deep water bioherms of the scleractinian coral *Lophelia pertusa* (L.) at 64°N on the Norwegian shelf: structure and associated megafauna. Sarsia 80:145–158

Mortensen P, Hovland MT, Fosså JH, Furevik DM (2001) Distribution, abundance and size of *Lophelia pertusa* coral reefs in mid-Norway in relation to seabed characteristics. J Mar Biol Assoc UK 81:1–17. https://doi.org/10.1017/S002531540100426X

Mortensen PB (2000) *Lophelia pertusa* (Scleractinia) in Norwegian waters. PhD-thesis, Department of Fisheries and Marine Biology, University of Bergen, Norway

Mucci A (1983) The solubility of calcite and aragonite in seawater at various salinities, temperatures and at one atmosphere pressure. Am J Sci 283:781–799

Osterloff J, Nilssen I, Järnegren J, Engeland TV, Buhl-Mortensen P, Nattkemper TW (2019) Computer vision enables short andlong-term analysis of *Lophelia pertusa* polyp behaviour and colour from an underwater observatory. Sci Rep 9:6578. https://doi.org/10.1038/s41598-019-41275-1

Philander SGH (1979) Upwelling in the Gulf of Guinea. J Mar Res 37:23–33

Pierrot D, Lewis E, Wallace DWR (2006) MS Excel program developed for CO_2 system calculations. ORNL/CDIAC-105a, Oak Ridge Natl. Lab, US Department of Energy https://cdiac.ess-dive.lbl.gov/ftp/co2sys/CO2SYS_calc_XLS_v2.1/

Portilho-Ramos RdC, Titschack J, Wienberg C, Siccha Rojas MG, Yokoyama Y, Hebbeln D (2022) Major environmental drivers determining life and death of cold-water corals through time. PLoS Biol 20(5):e3001628. https://doi.org/10.1371/journal.pbio.3001628

Pörtner H-O, Karl DM, Boyd PW, Cheung WWL, Lluch-Cota SE, Nojiri Y, Schmidt DN, Zavialov PO (2014) Ocean systems. In: Field CB, Barros VR, Dokken DJ, Mach KJ, Mastrandrea MD, Bilir TE, Chatterjee M et al (eds) Climate Change 2014 : Impacts, adaptation, and vulnerability Part A: Global and sectoral aspects Contribution of Working Group II to the Fifth Assessment Report of the Intergovernmental Panel on Climate Change. Cambridge University Press, Cambridge UK New York USA, pp 411–484

Reynolds RW, Smith TM, Liu C, Chelton DB, Casey KS, Schlax MG (2007) Daily High-Resolution-Blended Analyses for Sea Surface Temperature. J Clim 20:5473–5496

Richardson P, Reverdin G (1987) Seasonal cycle of velocity in the Atlantic North Equatorial Countercurren as measured by surface drifter, current meters, and ship drifts. J Geophys Res 92(C4):3691–3708

Roberts JM, Wheeler AJ, Freiwald A (2006) Reefs of the deep: the biology and geology of cold-water coral ecosystems. Science 312(5773):543–547. https://doi.org/10.1126/science.111986

Rokoengen K, Østmo SR (1985) Shallow geology off Fedje, western Norway. IKU Report 24. 24.1459/01/25, 20 pp

Schröder-Ritzrau A, Freiwald A, Mangini A (2005) U/Th-dating of deep-water corals from the eastern North Atlantic and the western Mediterranean Sea. In: Freiwald A, Roberts JM 8eds) Cold-Water Corals and Ecosystems. Erlangen Earth Conference Series. Springer, Berlin, Heidelberg. https://doi.org/10.1007/3-540-27673-4_8

Spalding C, Finnegan S, Fischer WW (2017) Energetic costs of calcification under ocean acidification. Global Biogeochem. Cycles 31:866–877. https://doi.org/10.1002/2016GB005597

Stramma L, Johnson GC, Sprintall J, Mohrholz V (2008) Expanding oxygen minimum zones in tropical oceans. Science 320(5876):655–658. https://doi.org/10.1126/science.1153847)

Strømgren T (1971) Vertical and horizontal distribution of *Lophelia pertusa* (Linne) in Trondheimsfjorden on the west coast of Norway. Det K Nor Vidensk Selsk Skr 6:1–9

Tamborrino L, Wienberg C, Titschack J, Wintersteller P, Mienis F et al (2019) Mid-Holocene extinction of cold-water corals on the Namibian shelf steered by the Benguela oxygen minimum zone. Geology 47(12):1185–1188. https://doi.org/10.1130/G46672.1

Teichert C (1958) Cold- and deep-water coral banks. Bull Am Assoc Pet Geol 42:1064–1082

Vélez-Belchí P, González-Carballo M, Pérez-Hernández MD, Hernández-Guerra A (2015) Open ocean temperature and salinity trends in the Canary Current Large Marine Ecosystem. In: Valdés L, Déniz-Gonzaléz I (eds) Oceanographic and biological features in the Canary Current Large Marine Ecosystem Intergovernmental Oceanographic Commission Technical Series 115. UNESCO, Paris, pp 299–308

Westphal H, Beuck L, Braun S, Freiwald A, Hanebuth et al. (2012) Phaeton – Paleoceanographic and paleo-climatic record on the Mauritanian Shelf. RV Maria S. Merian Cruise MSM16/3, Bremerhaven – Mindelo, 13.10.–20.11.2010. 53 pp

Wheeler AJ, Beyer A, Freiwald A, de Haas H, Huvenne VAI, Kozachenko M, Olu-Le Roy K, Opderbecke J (2007) Morphology and environment of cold-water coral carbonate mounds on the NW European margin. Int J Earth Sci 96:37–56. https://doi.org/10.1007/s00531-006-0130-6

Wiafe G, Nyadjro ES (2015) Satellite observations of upwelling in the Gulf of Guinea. IEEE Geosci Remote Sens Lett 12(2):1066–1070

Wienberg C, Titschack J, Freiwald F, Frank N, Lundälv T, Taviani M, Beuck L, Schröder-Ritzrau A, Krengel T, Hebbeln D (2018) The giant Mauritanian cold-water coral mound province: Oxygen control on coral mound formation. Quat Sci Rev 185:135–152

Zibrowius HW (1980) Les scléractiniaires de la Méditerranée et de l'Atlantique nordoriental. Mémoires de l'Institut océanographique 11 Monaco Institut océanographic. Description 3:284